Ocean Engineering 109 (2015) 635–653

Contents lists available at ScienceDirect

Ocean Engineering

journal homepage: www.elsevier.com/locate/oceaneng

Dynamic orifice flow model and compartment models for flooding simulation of a damaged ship

Gyeong Joong Lee

KRISO, 32, Yuseong-daero 1312 beon-gil, Yuseong-gu, Daejeon 305-343, Republic of Korea

ARTICLE INFO

Article history:
Received 3 January 2015
Accepted 29 September 2015
Available online 22 October 2015

Keywords:
Orifice equation
Flooding
Air compressibility
Damaged ship
Fully flooded compartment

ABSTRACT

When a damaged ship floods, flows of water and air move from one compartment to another, or to and from the outside. There are two main difficulties in simulation of such flooding. One is the effect of air, and the other is the calculation of pressure in a complex system of openings involving a large number of compartments. The air plays a crucial role in the flooding of some compartments, and the presence of air slows the rate of flooding in vented compartments. However, taking into account the effect of air results in 'ripples' of pressure fluctuation. Some other unusual difficulties arise, when many compartments are flooded.

In this paper, new models for vented compartments and an accumulator model were proposed, which can adjust the inner pressure automatically, even for systems with many compartments and openings, especially for fully flooded compartments. The dynamic-orifice equation was investigated for use in the case of large openings, so that the ripples in the air pressure that had been caused by the square-root singularity of the existing orifice equation could be eliminated. Application to a recent real accident showed the usefulness of the proposed models.

1. Introduction

While the number of flooding and sinking accidents is relatively small, they often lead to the tragic loss of personnel. Therefore, better knowledge about the processes that occur during flooding and sinking is required, and optimal response measures should be prepared according to the results of the study. For this purpose, a great deal of research about flooding has been conducted for specific real accidents, and safety assessments have been conducted during ship design, in anticipation of possible damage in the field.

The flooding simulation of a damaged ship seems to have been started by Spouge (1986), when he investigated the sinking of the Ro-Ro Ferry 'EUROPEAN GATEWAY'. He used a hydraulic-flow model to calculate the flood rate, and used an empirical formula to determine the center-of-gravity of the floodwater and its movement in transient asymmetric flooding stage. Sen and Konstantinidis (1987) developed his method further, and they obtained the position of the center-of-gravity by assuming the free surface always remains horizontal. Later, to take into account the dynamic effect of the floodwater, Papanikolaou et al. (2000) developed the method of lumped mass. A flow equation for shallow water and the movement of point mass followed (Chang and Blume, 1998; Chang, 1999). Computational fluid dynamics followed (van't Veer and de Kat, 2000; Woodburn et al., 2002; Cho et al., 2005); then the depth-averaged Euler equation was introduced (Lee, 2010). In relating the air flow and its compressibility, Palazzi and de Kat (2004) compared the results of model experiments and simulations of a damaged ship in which the entrapped air and its flow-out through vents were considered. Ruponen et al (2013) conducted a series of full-scale experiments for flooding of a tank with restricted ventilation level and compared these results with corresponding time-domain flooding simulations.

Until now, the hydraulic orifice equation has been used to obtain the flow between compartments. For the application of this equation, the following assumptions are required: incompressible fluid, inviscid fluid, steady conditions, and small openings (area). Among these, the assumptions of incompressible and inviscid fluid seem reasonable for seawater but for air, the incompressibility assumption may cause problems. However, the most troublesome assumption is that steady state: the flow velocity can change instantly as the pressure changes. Furthermore, in the case of small pressure differences, the application of this equation results in numerical instability because of the nature of square root function. This will be shown in detail later. Lee (2014) newly derived the dynamic-orifice equation from the basic equations of fluid mechanics. In this study, the property of this dynamic-orifice equation was investigated, and the sample calculations with analysis were given. This new version of the equation can be applied to unsteady states, and can eliminate the above-mentioned problems.

E-mail address: gjlee@kriso.re.kr

http://dx.doi.org/10.1016/j.oceaneng.2015.09.051

Another problem that occurs in the simulation of ship flooding, involves the calculation of the pressure in each compartment, when many compartments are connected to each other in complicated ways. This problem has been addressed previously (van't Veer et al., 2002, 2004; Ikeda et al., 2004; Vassalos et al., 2005). The most important thing is the determining a reference pressure for use in each compartment. Ruponen (2006) proposed a pressure-correction method that satisfied the mass-conservation law in order to determine the pressures of water and air in each compartment. He made a comprehensive study of this problem and validated his method using model tests (Ruponen, 2007). However, because his method determines the pressure by iteration, there was a convergence problem such as the number of iterations and the under-relaxation, and the iterations may not converge in some cases. He pointed out that the number of iterations goes larger for the inclusion of air flow, and pointed out that the final equilibrium condition may cause convergence problem with a long time step because of the small time derivatives of the water and air pressures. Dankowski (2013) simplified Ruponen's method especially for a fully flooded compartment, he used the non-linear equation drawn from the mass conservation law and solved it by iteration. And he investigated various real accidents. In our study, new models for vented compartments and an accumulator model were proposed, which can adjust the reference pressure automatically, even for systems with many compartments and openings, especially for fully flooded compartments.

2. Re-analysis of the orifice equation

In many studies, the following 'orifice equation' has been used in calculating the flow through an opening.

$$q = \rho C_D A v = \rho C_D A \sqrt{\frac{2\Delta p}{\rho}} \tag{1}$$

where, q and ρ are the mass flux and density of the flow through the opening, v is the velocity at the opening, A the area of the opening, Δp the pressure difference, and C_D the discharge coefficient. The above orifice equation was derived from the steady Bernoulli's equation.

In this section, the problem related to the above equation will be investigated, and we investigate a new equation that includes the dynamic effect. Then we verify its effectiveness and applicability.

2.1. Hydraulic orifice equation

Bernoulli's equation can be applied to the flow of an incompressible, inviscid fluid in steady state along a stream line. Bernoulli's equation and the continuity equation used for Fig. 1 are Eqs. (2) and (3), respectively.

$$\frac{p_0}{\rho} + \frac{1}{2}V_0^2 + g z_0 = \frac{p_1}{\rho} + \frac{1}{2}V_1^2 + g z_1 \tag{2}$$

$$A_0 V_0 = A_1 V_1 \tag{3}$$

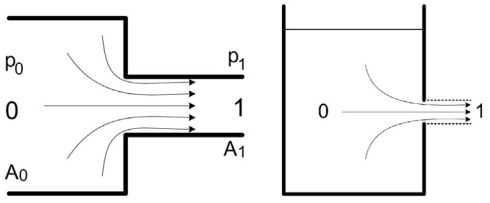

Fig. 1. Orifice and stream lines.

where, g is the gravitational acceleration, z the height of the position, the subscripts '0' and '1' indicate the orientation (position), the fluid flows from side '0' to side '1'. The total speed of the flow is the square root of the component velocity squared, $V = \sqrt{u^2 + v^2 + w^2}$. If the area of side '0' is large, and the height difference vanishes, the flow velocity through the orifice can be expressed as in Eq. (4) from Eqs. (2) and (3),

$$V_1 = \sqrt{\frac{2}{\rho}\Delta p} \tag{4}$$

The flux can then be obtained by multiplying the area of orifice, fluid density, and the discharge coefficient.

$$q = C_D \rho A \sqrt{\frac{2\Delta p}{\rho}} \tag{5}$$

The discharge coefficient C_D is related to the inlet/outlet shape, and the Reynolds number. Usually for an orifice with right-angled edges, a discharge coefficient of 0.6–0.7 is used.

Eq. (5) has a singular behavior of the square root function for small pressure differences. The rate of change with respect to the pressure difference, goes to infinity as the pressure difference goes to zero. Because of this, an unrealistic oscillation takes place when the pressure difference is small (as for an opening between two compartments with no other openings), while there is no problem when the pressure difference is large. This phenomenon of square root instability is explained in detail in Appendix B. Thus, the hydraulic orifice Eq. (5) is for a large pressure difference, subject to the assumptions stated previously (incompressible flow, and steady state condition).

2.2. Dynamic orifice equation

There are two problems with the hydraulic orifice equation. One is that it applies to steady state conditions. The second is that it applied orifices of small cross-section (area). In order to conduct a time-domain flooding simulation, it is required to include the dynamic effect, and to expand the applicability to include orifices of large area. Let us shortly introduce the work of Lee (2014), derivation of a new dynamic orifice equation. The momentum conservation law can be represented by the Euler equation for an incompressible, inviscid fluid (Eqs. (6) and (6′)).

$$\frac{\partial \vec{v}}{\partial t} + \left(\vec{v}\cdot\nabla\right)\vec{v} = \vec{F} - \frac{1}{\rho}\nabla p \tag{6}$$

$$\frac{\partial \vec{v}}{\partial t} + \frac{1}{2}\nabla(\vec{v}\cdot\vec{v}) = \vec{F} - \frac{1}{\rho}\nabla p \tag{6′}$$

where, $\vec{v}$ is a velocity vector, p the pressure, ρ the density of fluid, and $\vec{F}$ is the body force, including gravity. The above two equations are the same for incompressible and inviscid fluid. In this study, the integral version of the Euler equation will be used, so the momentum conservation law can be represented as in Eqs. (7) and (7′) for a specific control volume.

$$\int_\Omega \frac{\partial}{\partial t}\left(\rho\vec{v}\right)dV + \int_{\partial\Omega}\rho\vec{v}\left(\vec{v}\cdot\vec{n}\right)dS = \int_\Omega \rho\vec{F}\,dV - \int_{\partial\Omega} p\vec{n}\,dS \tag{7}$$

$$\int_\Omega \frac{\partial}{\partial t}\left(\rho\vec{v}\right)dV + \frac{1}{2}\int_{\partial\Omega}\rho\left(\vec{v}\cdot\vec{v}\right)\vec{n}\,dS = \int_\Omega \rho\vec{F}\,dV - \int_{\partial\Omega} p\vec{n}\,dS \tag{7′}$$

where, Ω is the control volume of concern, and $\partial\Omega$ is the boundary of the control volume. The orientation of the normal vector is outward normal.

Fig. 2 shows the orifice and the overall shape of the control volume, where R is the distance from the center of orifice and is chosen to be large so that the flow velocity at that distance will be

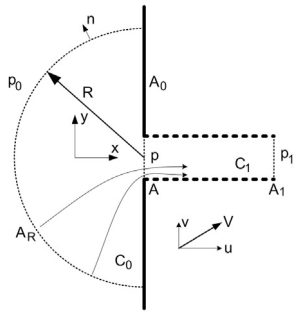

Fig. 2. Orifice, control volumes and related parameters.

small enough. On the boundary, A_R, the pressure is constant as p_0, and the flow velocity is parallel to the normal vector. Let us represent the velocity vector as $v^{\rightarrow}$, the velocity normal to orifice as u, and the total velocity as $V=\sqrt{u^2+v^2+w^2}$, here and after. At the right side of the orifice, the velocity and pressure are assumed to be constantly distributed. The area of the orifice is $A=A_1$, the area of the wall in which the orifice exists is A_0. The control volumes on the left and right are C_0 and C_1, respectively. The velocity components, excluding u, are asymmetric about the centerline of the orifice.

Applying the mass and momentum conservation law to the control volume C_0 and C_1, we can obtain the resulting Eq. (8) which relates the velocity at the orifice and the pressure difference. (Lee (2014) finally got Eq. (8) for the dynamic-orifice equation. The details of the derivation are attached in Appendix A.)

$$\frac{\sqrt{A}}{2}\frac{\partial \overline{u}}{\partial t}+\frac{7}{8}(\overline{u})^2=\frac{(p_0-p_1)}{\rho} \tag{8}$$

where, u is the average normal velocity at the orifice. The final velocity for a steady state of the above equation is:

$$\overline{u}_f=\sqrt{\frac{8}{7}\frac{(p_0-p_1)}{\rho}} \tag{9}$$

This final steady state value is less than that provided by Eq. (4). As briefly explained previously, the velocity from Eq. (4) is the total velocity, and that of Eq. (9) is the normal velocity at the orifice. It is reasonable to use the normal velocity for the calculation of flux through an orifice. Comparing Eqs. (4) and (9), it can be seen that the theoretical value of the contraction coefficient of a circular orifice with right-angle edge, is $\sqrt{4/7}\cong 0.756$ for an inviscid fluid. We can obtain the initial rate of velocity (i.e., initial acceleration) from rest using Eq. (8).

$$\frac{\partial \overline{u}}{\partial t}|_{t=0}=\frac{1}{\sqrt{A}}\frac{2(p_0-p_1)}{\rho} \tag{10}$$

The time to reach final velocity using the initial rate of change would be:

$$T=\frac{\overline{u}_f}{d\overline{u}/dt|_{t=0}}=2\sqrt{\frac{A}{7}}\sqrt{\frac{\rho}{2(p_0-p_1)}} \tag{11}$$

Fig. 3 shows the velocity rise with respect to time from Eq. (8), when the pressure difference is a step-function.

The velocity reaches 0.765 of the final velocity at $t=T$, 0.965 at $t=2T$, and 0.99 at $t=3T$. One can obtain the velocity by integrating Eq. (8) for small size of time step compared with T. From Fig. 3, the numerical time integration using Eqs. (8) or (10) seems not to be desirable if the size of time step of the simulation is larger than T. For that case, one can use Eq. (9) rather than 8. Here, T (from Eq. 11) becomes larger as the pressure difference becomes smaller. This means that the dynamic model works for the case of small pressure differences, even if we use a fixed size of time step.

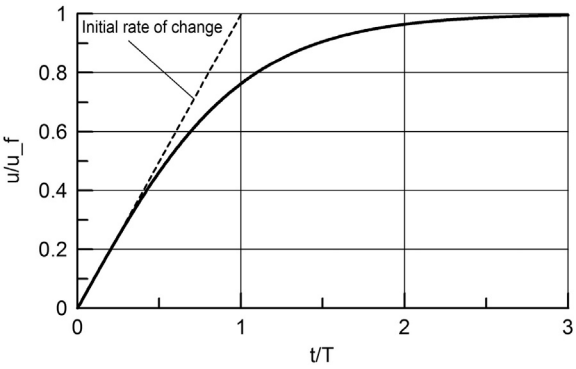

Fig. 3. Orifice velocity behavior when the pressure difference is a step function.

For the discharge coefficient, the use of $C_D/\sqrt{4/7}$ is desirable because of the difference between the normal velocity and total velocity in Eqs. (9) and (4). The density in Eq. (8) should be determined according to the sign of the velocity, not the sign of the pressure difference. Eq. (8) stands for positive velocity only, and we can modify the equation a little bit for both directions.

$$\begin{aligned}&\frac{\sqrt{A}}{2}\frac{\partial \overline{u}}{\partial t}+\frac{7}{8}\overline{u}|u|=\frac{(p_0-p_1)}{\rho}\\ &\text{if } \overline{u}\geq 0, \rho=\rho_0\\ &\text{if } \overline{u}<0, \rho=\rho_1\end{aligned} \tag{12}$$

2.3. Large opening

The pressure difference can vary across the orifice when it is large. If the pressure difference is constant over the orifice area, Eqs. (4) and (12) can give the flow velocity. If it varies, it is possible to obtain the flow by solving the Euler equation or the Navier–Stokes equation. However, this is impractical for a system with many compartments and orifices. A more practical way is to integrate the expression over the orifice area in order to obtain the flux through the orifice. The hydraulic orifice Eqs. (4) and (5) do not include the concept of average velocity, but for practical calculation, one can use the average concept of velocity by integrating them over the orifice area. Meanwhile, the dynamic orifice Eq. (12) uses the average velocity, so it creates no logical problem to integrate the pressure difference in order to get the forces acting on the surrounding fluid. Therefore, the average velocities could be obtained using the following equations, and multiplying the orifice area gives the flux.

$$V=\frac{1}{A}\int_A\sqrt{\frac{2}{\rho}\Delta p}\,dA=\frac{1}{A}\sqrt{\frac{2}{\rho}}\int_A\sqrt{\Delta p}dA \tag{13}$$

$$\frac{\sqrt{A}}{2}\frac{\partial \overline{u}}{\partial t}+\frac{7}{8}\overline{u}|\overline{u}|=\frac{1}{\rho A}\int_A\Delta p dA \tag{14}$$

where, $\Delta p=p_0-p_1$ is the pressure difference across the orifice. The mass flux can be obtained by the following equations. (The subscripts 'h' and 'd' mean the flux from the hydraulic orifice equation and dynamic orifice equation, respectively.)

$$q_h=\rho C_D A V \tag{15}$$

$$q_d=\rho C_D^{'} A\overline{u} \tag{16}$$

where the value of C_D is from the hydraulic experiment, so use $C_D^{'}$ as $C_D/\sqrt{4/7}$.

Another big problem with larger openings is the fact that the free surface may lie upon cross section of the orifice. Following are a number of cases (Fig. 4) that could occur, depending on the height of the free surface, and the substances on both sides of the orifice.

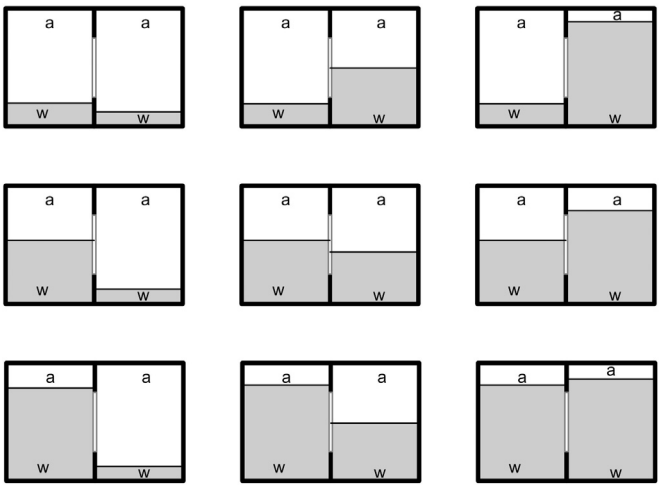

Fig. 4. Orifice and adjacent substances ('a' is air, 'w' is water).

As shown in Fig. 4, these cases can be classified into four boundary types (within the orifice) according to the substances in contact: air–air, air–water, water–air, and water–water. The integration of Eqs. (13) and (14) can be obtained by dividing the orifice area into sub-regions so that each sub-region has one type of material boundary, then integrating the Eqs. (13) and (14) over each sub-region, and adding the results.

Regarding the shape of the openings, many have long, narrow shapes (e.g., doors and gaps). In these cases, one-dimensional (1-D) integration may be helpful, but for other cases the integration should be done in 2-D.

In order to calculate the flow through an opening, there is a need for several definitions. First, the identification of the compartment of interest is needed because the opening connects two compartments; thus, we have Compartment 0 and Compartment 1. This identification may be provided by adding the subscript '0' or '1'. The velocity is defined as positive when the flow is from Compartment 0 to Compartment 1; whereas, negative velocity means flow in the opposite direction. Compartment 0 is called the 'donor'; Compartment 1 is the 'acceptor'. The subscripts '*w*' and '*a*' refer to the substances water and air, respectively.

The two substances can flow through the opening simultaneously, so the flux may be identified by adding subscript as follows,

q_{ha}: mass flux of air using hydraulic orifice equation
q_{hw}: mass flux of water using hydraulic orifice equation
q_{da}: mass flux of air using dynamic orifice equation
q_{dw}: mass flux of water using dynamic orifice equation

First, let us divide the opening area into sub-regions with one of the four types of boundary (i.e., 'air–air', 'air–water', 'water–air', and 'water–water'). If the sign of the pressure difference changes in any sub-region, this sub-region is divided into two sub-regions so that each sub-region has a distinct sign of pressure difference, and one boundary type. For each sub-region, calculate the following integrals,

$$I_i = \int_{A_i} sgn(\Delta p)\sqrt{|\Delta p|}\,dA \tag{17}$$

$$J_i = \int_{A_i} \Delta p\,dA \tag{18}$$

$$A_i = \int_{A_i} dA \tag{19}$$

where, $sgn(\Delta p)$ is the sign of Δp. Because the integrand has one sign, the sign of the integral is the same as the sign of the pressure difference.

The mass flux can be calculated using the above integrals, if we use the hydraulic orifice Eqs. (20) and (21).

$$q_{ha} = \sum_i \begin{cases} \rho_{a0} C_D \sqrt{2/\rho_{a0}}\, I_i & for\ I_i \geq 0, and\ donor\ is\ air \\ \rho_{a1} C_D \sqrt{2/\rho_{a1}}\, I_i & for\ I_i < 0, and\ acceptor\ is\ air \end{cases} \tag{20}$$

$$q_{hw} = \sum_i \begin{cases} \rho_{w0} C_D \sqrt{2/\rho_{w0}}\, I_i & for\ I_i \geq 0, and\ donor\ is\ water \\ \rho_{w1} C_D \sqrt{2/\rho_{w1}}\, I_i & for\ I_i < 0, and\ acceptor\ is\ water \end{cases} \tag{21}$$

To use the dynamic orifice Eq. (14), the calculation should be done according to the sign of the velocity not the sign of the pressure difference. Because the velocity is the unknown, two cases (positive and negative) should be prepared. Thus,

For air – air, $J_{Pa} = \sum_i J_i, A_{Pa} = \sum_i A_i$

$J_{Ma} = \sum_i J_i, A_{Ma} = \sum_i A_i$

For water – water, $J_{Pw} = \sum_i J_i, A_{Pw} = \sum_i A_i$

$J_{Mw} = \sum_i J_i, A_{Mw} = \sum_i A_i$

For air – water, $J_{Pa} = \sum_i J_i, A_{Pa} = \sum_i A_i, \text{if } J_i \geq 0$

$J_{Mw} = \sum_i J_i, A_{Mw} = \sum_i A_i, \text{if } J_i < 0$

For water – air, $J_{Pw} = \sum_i J_i, A_{Pw} = \sum_i A_i, \text{if } J_i \geq 0$

$J_{Ma} = \sum_i J_i, A_{Ma} = \sum_i A_i, \text{if } J_i < 0$

According to the sign of the velocity, the following equations give the averaged water and air velocities.

$$\frac{\sqrt{A_{Xa}}}{2}\frac{\partial(\overline{u})_a}{\partial t} + \frac{7}{8}\overline{u}|\overline{u}|_a = \frac{1}{\rho A_{Xa}} J_{Xa} \tag{22}$$

$$\frac{\sqrt{A_{Xw}}}{2}\frac{\partial(\overline{u})_w}{\partial t} + \frac{7}{8}\overline{u}|\overline{u}|_w = \frac{1}{\rho A_{Xw}} J_{Xw} \tag{22'}$$

Eq. (22) is for the air flow, and (22′) is for the water flow. In the above equation '*X*' is '*P*' if the velocity is positive; while '*M*' is negative. The mass flux can be obtained by the following equations.

$$q_{da} = \rho_a C'_D A_a (\overline{u})_a \tag{23}$$

$$q_{dw} = \rho_w C'_D A_w (\overline{u})_w \tag{23'}$$

In some cases, the force acting on a door is required to determine when the door will collapse; the force can be obtained by simply adding all J_i.

2.3.1. 1-D opening

Sometimes, it is convenient to neglect the variation of the pressure difference along width and to integrate it along the height, for a door or its gap, as shown in Fig. 5.

The integration of Eqs. (17)–(19) can be carried out analytically by assuming the linear variation of pressure difference in each sub-region. For the *i*-th sub-region,$(h_i \leq h < h_{i+1})$ the pressure difference can be represented as,

$$\Delta p = a_i(h - h_i) + b_i$$
$$b_i = \Delta p_i\ , a_i = (\Delta p_{i+1} - \Delta p_i)/(h_{i+1} - h_i)$$

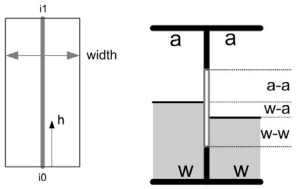

Fig. 5. Shape of 1-D opening and sub-regions of orifice.

Then, substitute the above into Eqs. (17) and (18), and integrate them analytically. The results of the integrations for $a_i = 0$ are:

$$I_i = sgn(\Delta p_i) w_0 \int_{h_i}^{h_{i+1}} (|\Delta p|)^{1/2} dh = sgn(\Delta p_i) w_0 (|\Delta p|)^{\frac{1}{2}} (h_{i+1} - h_i) \tag{24}$$

$$J_i = w_0 \int_{h_i}^{h_{i+1}} \Delta p dh = w_0 \Delta p (h_{i+1} - h_i) \tag{25}$$

$$A_i = w_0 \int_{h_i}^{h_{i+1}} dh = w_0 (h_{i+1} - h_i) \tag{26}$$

and for $a_i \neq 0$,

$$I_i = sgn(\Delta p_i) w_0 \int_{h_i}^{h_{i+1}} (|\Delta p|)^{\frac{1}{2}} dh = sgn(\Delta p_i) w_0 \frac{2}{3a_i} \left[\Delta p (|\Delta p|)^{\frac{1}{2}} \right]_i^{i+1} \tag{27}$$

$$J_i = w_0 \int_{h_i}^{h_{i+1}} \Delta p dh = w_0 \frac{1}{2a_i} \left[(\Delta p)^2 \right]_i^{i+1} \tag{28}$$

$$A_i = w_0 \int_{h_i}^{h_{i+1}} dh = w_0 (h_{i+1} - h_i) \tag{29}$$

where, $[\,]_i^{i+1}$ means the subtraction of i indexed value from $i+1$ indexed value. The above expression was drawn to be independent of the sign of the pressure difference. The resulting equations (from Eqs. ((24)–29)) can be used for any inclination angle if one use the local coordinate fixed in the opening.

2.3.2. 2-D opening

For the general shape of an opening, the integration would be carried out in 2-D. Let us divide the opening area into sub-regions as explained previously, which can be represented as a closed polynomial. Next, integrate them over each sub-region using the Stokes theorem. Let us fit the pressure difference by bi-linear interpolation as in Eq. (30).

$$\Delta p = ax + by + c \tag{30}$$

Three constants a, b, and c can be found from three conditions at three vertices of that polynomial.

$$\begin{aligned} \Delta p_0 &= ax_0 + by_0 + c \\ \Delta p_1 &= ax_1 + by_1 + c \\ \Delta p_2 &= ax_2 + by_2 + c \end{aligned} \tag{31}$$

Let us change the area integral to the contour integral, along the contour C_i using Stokes theorem.

$$I_i = sgn(\Delta p) \iint_{R_i} \sqrt{|\Delta p|} dx dy = \frac{2}{3a} \oint_{C_i} |\Delta p|^{2/3} dy \tag{32}$$

$$J_i = \iint_{R_i} \Delta p dx dy = \frac{1}{2a} \oint_{C_i} (\Delta p)^2 dy \tag{33}$$

$$A_i = \iint_{R_i} dx dy = \oint_{C_i} x dy \tag{34}$$

On the j-th line segment of the i-th sub-region, the following geometric relation exists.

$$x = b_{xj} y + c_{xj}, \quad b_{xj} = \frac{x_{j+1} - x_j}{y_{j+1} - y_j}, \quad c_{xj} = x_j - \frac{x_{j+1} - x_j}{y_{j+1} - y_j} y_j$$

Therefore, the pressure difference (30) can be expressed as follows on the j-th line segment.

$$\Delta p = ax + by + c = b_j' y + c_j'$$

$$b_j' = b + a b_{xj}, c_j' = c + a c_{xj}$$

If we integrate Eq. (32), the results are (for $a \neq 0$),

$$I_i = sgn(\Delta p) \frac{2}{3a} \sum_j \begin{cases} \frac{2}{5b_j'} \left[(\Delta p)^2 (|\Delta p|)^{1/2} \right]_j^{j+1} & for\ b_j' \neq 0 \\ (\Delta p) (|\Delta p|)^{1/2} \left(y_{j+1} - y_j \right) & for\ b_j' = 0 \end{cases} \tag{35}$$

and for $a = 0$, $(b_j' = b,\ c_j' = c)$

$$I_i = sgn(\Delta p) \sum_j \begin{cases} \frac{2}{15b^2} \left[(5bx - 2b_{xj} \Delta p)(\Delta p)(|\Delta p|)^{1/2} \right]_j^{j+1} & for\ b \neq 0 \\ \frac{1}{2} (|\Delta p|)^{1/2} (x_{j+1} + x_j) \left(y_{j+1} - y_j \right) & for\ b = 0 \end{cases} \tag{36}$$

The results of Eq. (33) are (for $a \neq 0$),

$$J_i = \frac{1}{2a} \sum_j \begin{cases} \frac{1}{3b_j'} \left[(\Delta p)^3 \right]_j^{j+1} & for\ b_j' \neq 0 \\ (\Delta p)^2 \left(y_{j+1} - y_j \right) & for\ b_j' = 0 \end{cases} \tag{37}$$

and for $a = 0$, $(b_j' = b, c_j' = c)$

$$J_i = \sum_j \begin{cases} \frac{1}{6b^2} \left[(3bx - b_x \Delta p)(\Delta p)^2 \right]_j^{j+1} & for b \neq 0 \\ \frac{1}{2} (\Delta p)(x_{j+1} + x_j) \left(y_{j+1} - y_j \right) & for b = 0 \end{cases} \tag{38}$$

The area, from Eq. (34), can be rewritten as follows.

$$A_i = \sum_j \frac{1}{2} (x_{j+1} + x_j)(y_{j+1} - y_j) \tag{39}$$

As in 1-D opening, the resulting equations (from Eqs. (35)–(39)) can be used for any inclination angle if one use the local coordinate fixed in the opening.

2.4. Sample application

Let us consider the case in which two compartments are adjacent, and an opening is located in the wall between them. The size of the compartment is 5 m (L) × 5 m (W) × 5 m (H), and there is no vent. The sample calculations were carried out for a point and a 1-D opening, the compressibility of air was included, and an isothermal process was assumed. The time integration scheme was Euler explicit method with the time interval of 0.01 s . And the result from the dynamic orifice equation was compared with that from the hydraulic orifice equation.

2.4.1. Comparison of point opening and 1-D opening

If the pressure difference is large across an opening, the flow characteristics are similar for a point opening and 1-D opening. However, for small pressure difference, there may be different flow characteristics. Let us set up model as in Fig. 6 in order to view this. For a point opening, the area of the opening is 1 m^2 and the location of the orifice 1 m from the bottom. A 1-D calculation was also made for the comparison, with the same area while the top of opening is apart 1 m from the bottom. The calculation cases are shown in Fig. 6.

The results are shown in Fig. 7 in comparison with 1-D calculation.

The filling ratio of Compartment 0 decreases with time, and the filling ratio of Compartment 1 increases. However, the results for the point-opening vary slowly, except in the initial stage, and the pressure in Compartment 0 oscillates. The flows of water and air are shown in Fig. 8.

In the initial stage, the pressure on the left side of opening is much higher than on the right side, so the water flows toward Compartment 1. As the water level in Compartment 0 goes down, the pressure goes down in Compartment 0 and goes up in Compartment 1. Around 2 s in time, the pressure difference (pressure in Compartment 0 minus pressure in Compartment 1 at the top of opening) goes small, and the flows rates show quite different behaviors. The flow of air exhibits many rapid small oscillations with the hydraulic orifice equation, while it exhibits intermittent large oscillations with the dynamic orifice equation. This affects the pressure fluctuation in Fig. 7. For 1-D openings, the water and air can flow simultaneously in opposite directions, the flow is smoother, and the filling ratio reaches the value we anticipated. In order to view the reason of the fluctuation of flows, the enlarged view with the pressure difference is helpful as in Fig. 9.

For a point opening using hydraulic orifice equation (top graph of Fig. 9), a positive pressure difference induces the water flow. At the moment in which the pressure difference is negative, the water-flow is blocked and the air-flow from Compartment 1 Compartment 0 takes place. At the very next time, the pressure difference becomes positive and the air-flow is blocked and water-flow from Compartment 0 to Compartment 1 takes place. After that, the pressure difference goes down as the water level in Compartment 0 goes down, and the

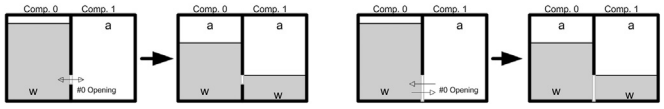

Fig. 6. Sample model for point opening (left two) and equivalent 1-D opening (right two) (In each pair of figures, the left figure shows the initial state, and the right figure shows the expected final state.).

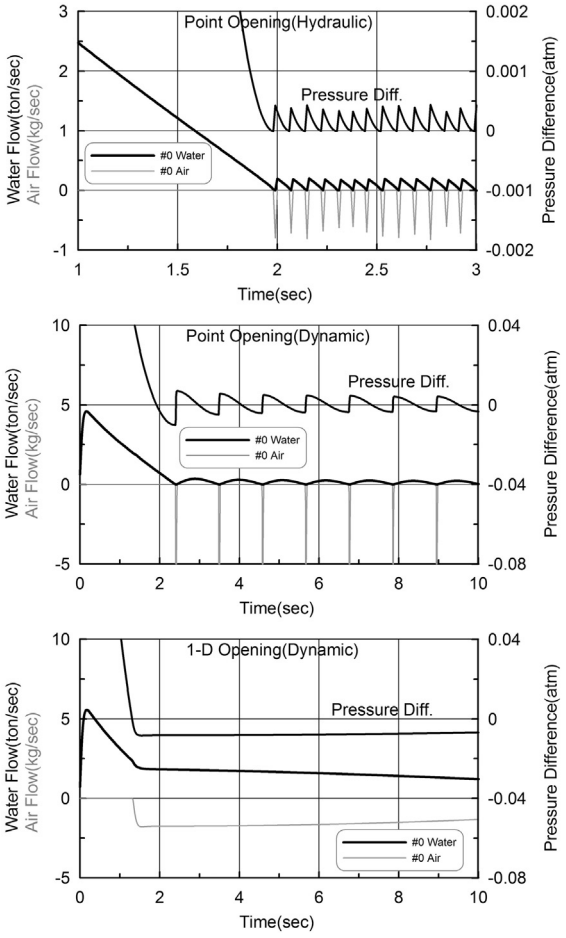

Fig. 9. Enlarged view of the pressure difference at the top of opening and flow rates (point opening (top and center) and 1-D opening (bottom)).

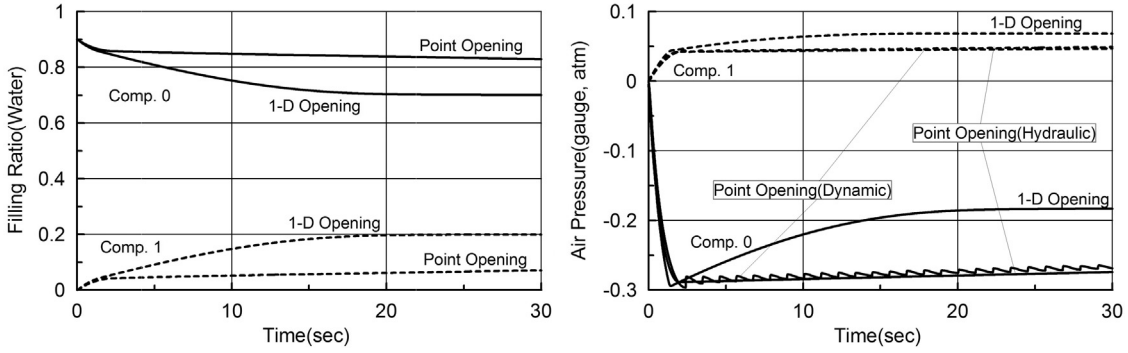

Fig. 7. Filling ratio (left) and the air pressure (right) in compartments with a point-opening.

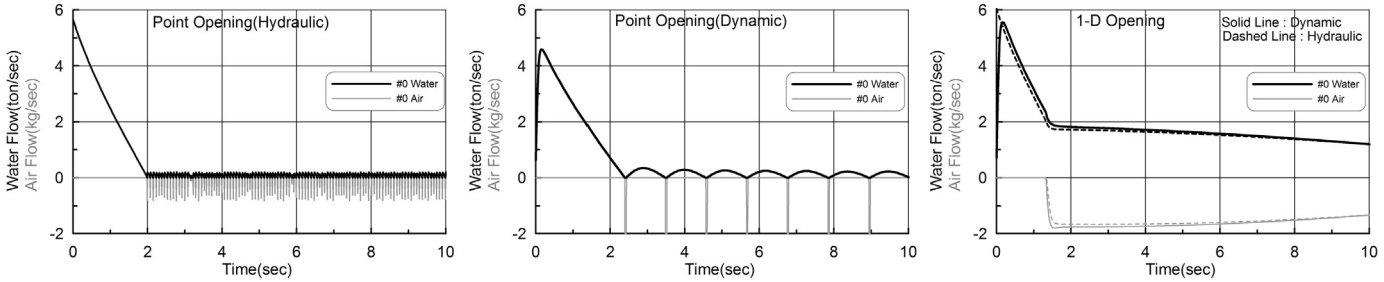

Fig. 8. Flow rates of water and air for point (left and center) and 1-D openings (right) (Positive value means the flow direction is from Compartment 0 to Compartment 1).

process explained above repeats again. For a point opening using dynamic orifice equation (center graph of Fig. 9), the air-flow takes place a little bit later after the pressure difference becomes negative, because of the dynamic effect of water flow. In this time, the amount of air-flow is large compared with that of hydraulics because of the large negative pressure difference, therefore the pressure difference jumps up to positive large value. The pressure and flow fluctuation are larger and smoother than in hydraulic equation. The above two phenomena of pressure fluctuations happen because a point opening allow the flow of only one substance at a time.

For a 1-D opening (bottom graph of Fig. 9), from the moment at which the pressure difference becomes negative, the air-flow occurs in the direction opposite to water-flow. And after, the water and air flow simultaneously in opposite directions. The pressure difference at the top of opening is negative, while it is positive at the bottom of opening because of the static pressure due to water height. Therefore the water could flow in some part of opening, and the air could flow in other part in opposite direction. From these results, we now know that point-openings should not be used when there is only one opening in a compartment.

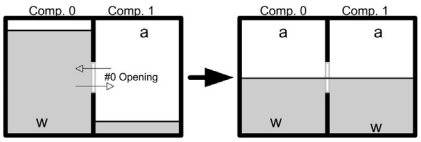

Fig. 10. Sample case: centered 1-D opening (The left figure shows the initial state, and the right figure shows the expected final state.).

2.4.2. *Comparison of hydraulic and dynamic orifice equation*

In order to view the effectiveness of the dynamic orifice equation, sample calculation was carried out for the case involving a 1-D opening in the middle of the wall (Fig. 10). In the expected final stage, the air in two compartments is connected through the upper part of the opening.

The results are shown in Fig. 11. The filling ratios and air pressures are similar, while the results from the dynamic orifice equation are a little bit faster. However, the air flows after 30 s are quite different from each other. The result from the hydraulic orifice equation starts to oscillate highly around 30 s; an enlarged view of this oscillation was drawn in Fig. 12. This oscillation is due to the numerical stability of the square root explained in Appendix A. However, the results from the dynamic orifice equation oscillated smoothly. This might be from an inertia effect.

The results from the sample calculations above show that the point opening should not be used for the cases with one opening in a compartment, and that the numerical instability takes place when the air in both compartments is connected through an opening. Surely, for the case of many compartments, the numerical instability due to the square-root function can ruin the flooding simulation. The dynamic orifice equation can solve this problem as it did in the above calculations.

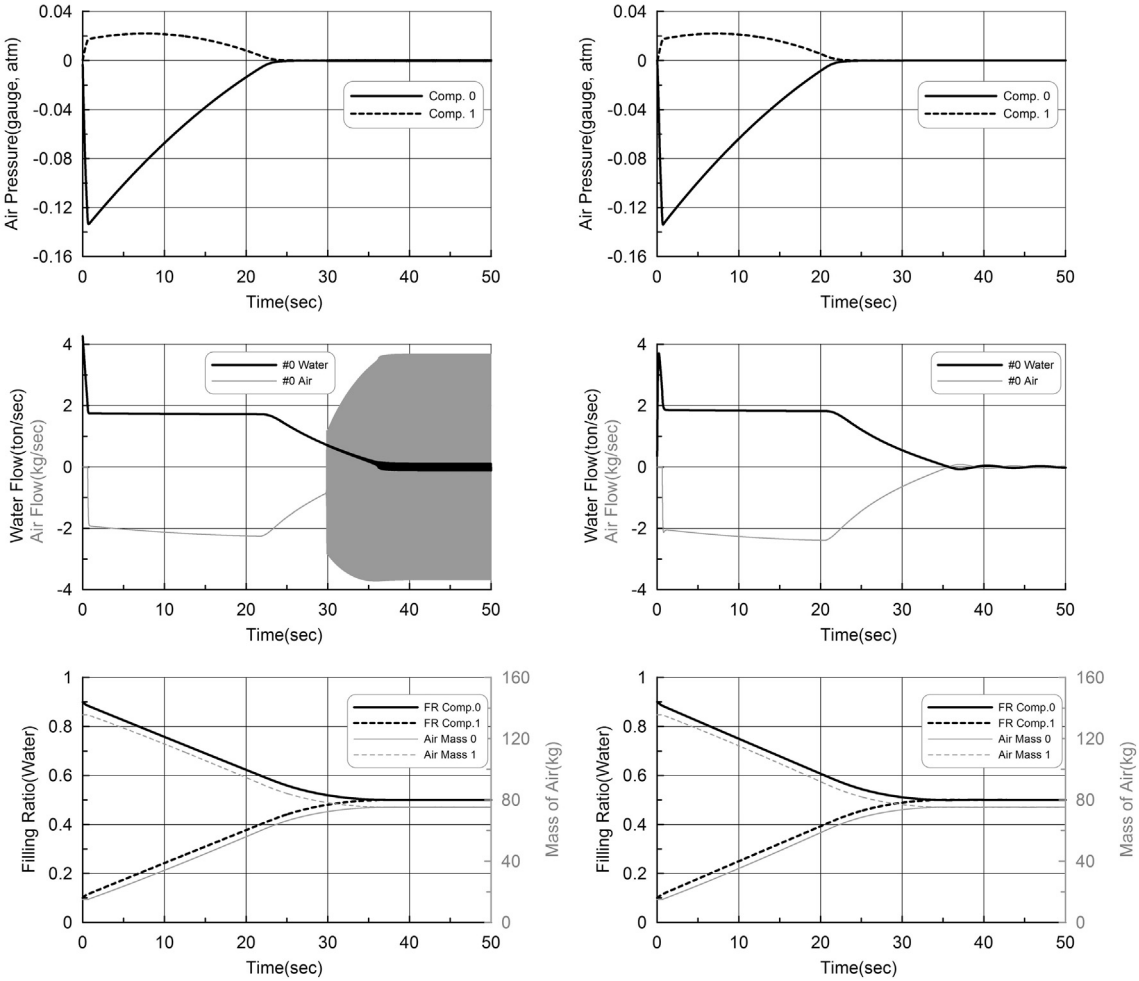

Fig. 11. Time simulation results for the sample case (centered 1-D opening), left – results from the hydraulic orifice equation, right – results from the dynamic one.

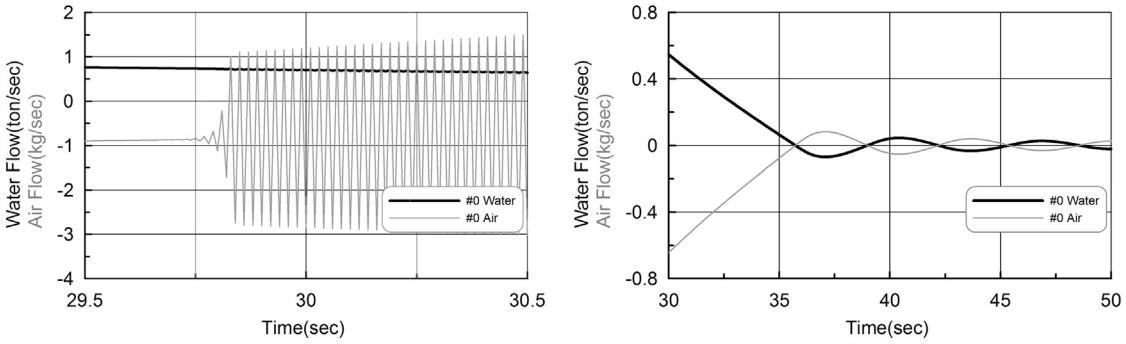

Fig. 12. Enlarged view of the flow rates of water and air: left–for hydraulic orifice equation, right – for the dynamic one).

3. Compartment model

If damage occurs in a ship with many rooms, like a passenger ship, the flows of floodwater and air through the inside passages is quite complicated. If we take the air compressibility into account, all routes for air flow should be modeled. But because the path of the air flow is so complex especially in the ventilation system, flooding simulations in many studies have been done without solving for the air flow. However, the air could block the flow of water into some compartments, and retard the flooding rate. In such a case, the air passage should be modeled as best as possible. It is manageable for the vent system of most compartments except for the complex ventilation system in the living quarter of a ship, in which it has no choice but simplification without losing the purpose of an analysis.

As stated in the introduction (Section 1), the most important thing is to provide the reference pressure in a compartment. If a compartment is partially filled with water, the reference pressure is the one on the free surface, i.e. the air pressure. The pressure below the free surface can be obtained by adding the pressure due to water depth, to the reference pressure. In fully water-filled compartment, there exist no free surface; so no air pressure. In such cases, selection of the reference pressure is a problem. Ruponen (2006, 2007) introduced the idea of water height pressure at each compartment to play the role of reference pressure in fully filled compartments. He drew the non-linear simultaneous equations for the reference pressures to satisfy the mass conservation law for each compartment. It is called the pressure-correction equation. However, it is complex and one should use iteration method to solve it. In some cases, the iterations would not converge, so under-relaxation was used. Dankowski (2013) ignored the air flow and its effect except for the entrapped air, so has a problem of the reference pressure only for the fully filled compartments. He solved the non-linear mass conservation equation by iteration. Ruponen and Dankowski began with a mass conservation law in order to indirectly obtain the pressure in a compartment; Ruponen applied the pressure-correction scheme and Dankowski directly solved the equation from mass conservation law. The difference should be noted is that Ruponen applied it to the entire set of compartments while Dankowski only to the fully filled compartments.

However, if we have an equation or tool which directly gives the reference pressure in a compartment, there is no need to worry about the mass conservation. If we solve the dynamic equation derived from the conservation law, the conservation will be satisfied intrinsically. The compartment that can be fully flooded is usually one with a vent. For this compartment, the mass conservation law will be satisfied if we count on the mass flowing through the air vent, that is, mass conservation for the compartment and vent, not the compartment only.

In this section, as a direct model to give the reference pressure, two new models were proposed for the compartment flow model. One is the method which counts on the mass in the vent and obtains the reference pressure for a fully filled compartment. The other is a virtual accumulator model that gives the pressure and can stabilize the excessive fluctuation of pressure in a compartment.

3.1. Basic compartment model

Consider a compartment in which all the openings, including vents, are well defined. The mass of water and air can be calculated as,

$$\dot{m}_w = q_w$$
$$\dot{m}_a = q_a \ (for\ m_a \geq 0) \tag{40}$$

where, m_w, m_a are the mass of water and air; q_w, q_a are the mass flux of each substance into the compartment through all openings. The volume charged by water V_w is calculated by m_w/ρ_w, then the remaining volume of the compartment is the volume charged by air V_a. The state equation of ideal gas gives the pressure of the air.

$$pV^{\gamma} = const. \quad \rightarrow \quad p_a = k_{atm}\rho_a^{\gamma} - p_{atm} \tag{41}$$

where, the density of air $\rho_a = m_a/V_a$, and the constant coefficient of the atmospheric condition $k_{atm} = p_{atm}/\rho_{atm}^{\gamma}$. The pressure p_a is the gauge pressure, and p_{atm} is the atmospheric pressure. About the ratio of specific heat γ, the value '1' is adequate for the case that the flooding is proceeded slowly (i.e., the slow compression, iso-thermal), and 7/5 for the case of rapid compression (iso-entropic).

3.2. Vented compartment model

A vented compartment is one from which the air can flow out, if the water flows into it, without actually describing the details of vent duct. If the vent area (cross-section) is large enough, the air is easily vented if the water flows in, so the air pressure is almost the same as atmospheric pressure. However, for a small vent area, the air would become compressed, so that the pressure of the air inside is greater than atmospheric pressure. The compartments can then be categorized into partially vented and fully vented compartments. Suppose a compartment which has a vent opening (area A_v) at the top and a damage opening (area A_d) at the bottom. The density change can be represented as

$$\rho_a = \frac{\dot{m}_a}{V_a} - \frac{m_a}{V_a^2}\dot{V}_a = \frac{m_a}{V_a^2}\left(-C_D A_v\sqrt{2p_a/\rho_a} + A_B\dot{h}\right) \tag{42}$$

where, A_B and h are the bottom area and rising rate of water respectively. The density will be reached to its maximum value when the above rate goes zero. The condition of equilibrium turns

out to be,

$$\frac{A_v}{A_B}=\frac{1}{C_D\sqrt{2p_a/\rho_a}}\dot{h}=\frac{1}{C_D\sqrt{2k_{atm}(1-\rho_{atm}/\rho_a)}}\dot{h} \tag{43}$$

On the other hand, the rising rate $\dot{h}$ can be represented using the water depth H at the damage opening as follows,

$$\dot{h}=A_d\sqrt{2gH}/A_B \tag{44}$$

Substitute this into Eq. (43),

$$\frac{A_v}{A_d}=\frac{\sqrt{2gH}}{C_D\sqrt{2k_{atm}(1-\rho_{atm}/\rho_a)}} \tag{45}$$

Assume C_D as 2/3, and substitute k_{atm} into the above equations,

$$\frac{A_v}{A_B}=\frac{0.003765}{\sqrt{1-\rho_{atm}/\rho_a}}\dot{h}$$
$$\frac{A_v}{A_d}=\frac{0.003765}{\sqrt{1-\rho_{atm}/\rho_a}}\sqrt{2gH} \tag{46}$$

If we want the density change is below 1%,

$$\frac{A_v}{A_B}\geq 0.03784\times\dot{h}$$
$$\frac{A_v}{A_d}\geq 0.03784\times\sqrt{2gH} \tag{47}$$

The above formula can give the criteria for the full ventilation. In order to suggest a criterion, the water depth of damage is assumed 10 m, and the free surface rising rate is assumed to be 0.3 m/s. And then we can categorize the compartment as fully vented if the vent area A_v satisfies the one of the following conditions.

$$A_v\geq 0.01\ \times(\text{top area})\cong 0.01\times\ (V_{max})^{2/3}$$
$$A_v\geq 0.5\ \times(\text{sum of all the area of water flow in}) \tag{48}$$

The criterion for a fully vented compartment could be suggested as a vent area greater than 1/100 of the top area. As a matter of fact, the assumed free surface rising rate and water depth using in drawing the criteria are not the absolute values, these may be altered by other situation and the researcher's choice.

When a compartment is not fully filled with water, the compartment flow model could be drawn from Eqs. (40) and (41).

For a fully vented compartment,

$$\dot{m}_w=q_w$$
$$V_w=m_w/\rho_w$$
$$p_a=0 \tag{49}$$

For a partially vented compartment,

$$\dot{m}_w=q_w$$
$$\dot{m}_a=q_a+q_{av}$$
$$q_{av}=\begin{cases}-C_D\rho_a A_v\sqrt{2p_a/\rho_a} & for\ p_a\geq 0\\ C_D\rho_{atm}A_v\sqrt{-2p_a/\rho_{atm}} & for\ p_a<0\end{cases}$$
$$V_w=m_w/\rho_w$$
$$V_a=V_{max}-V_w$$
$$\rho_a=m_a/V_a$$
$$p_a=k_{atm}\rho_a^{\gamma}-p_{atm} \tag{50}$$

where, q_{av} is the air mass flux through vent.

There is no problem in calculating the flows of water and air, and the pressure, if air remains in the compartment, as in Fig. 13 (left). If, however, all the air flows out (Fig. 13, right) there is no means to calculate the pressure in it without comparing the surrounding pressure (i.e., there is no reference pressure). Even in this case, water can enter the compartment; the mass conservation law seems to be violated without considering the flow through the vent. If the same amount of water is understood to flow out through the vent, the mass conservation law is satisfied. We found a way to designate a reference pressure, considering the pressure at the position of the vent. For this purpose, we propose the following 'vent water column' concept for vented compartment model (Fig. 14).

For the real vent duct (or ducts) substitute a simple vertical (virtual) vent (i.e., introduce a vertical air–water column at the top of the compartment). For the case of partial filling, there is no problem, and the reference pressure is the air pressure. Even for the case of full filling, the water can flow into the compartment; the surplus water flows up through the vertical vent. The surplus water fills the vertical vent and the top surface goes up to the free surface, and the reference pressure will be set to the pressure corresponding to the height of the water column in the vertical vent. If more water flows into it, the height of water column will be higher than the free surface, and the reference pressure will be higher than the surrounding compartment. If so, the water in that compartment could flow out to another compartment, and the height of water column could be lowered (that is, the reference pressure will be set to the correct value automatically). The above explanations reflect real situations well, and the conservation of mass is satisfied.

Let us introduce 'vent water column' concept in order to obtain the reference pressure for a fully filled compartment. For $V_w/V_{max}\geq 1$ (i.e. fully water-filled), the water height and reference pressure can be obtained from Eq. (51).

$$V_w=V_{max}$$
$$\dot{V}_v=q_w/\rho_w$$
$$h_v=\ V_v/A_v$$
$$p_a=\rho_w g h_v+p_{vent} \tag{51}$$

where, h_v, V_v are the height and volume of the water column in the vertical vent, respectively. And p_{vent} is the pressure loss due to the flow through the vent. It can be represented by the equation $p_{vent}=1/2\,\rho\,v^2$, in which the velocity and density is assumed to be those of the air flowing through the vent. At the moment when the compartment is just fully filled, the pressure of air (i.e., the reference pressure) has a jump to p_{vent}. If we use the density and velocity of the water, this gives very large value at that moment, whereas it will soon be balanced with the adjacent compartment. So it is recommended to use the density and velocity of the air through the vent, and add some damping to it. If the vent area is large as in fully vented, the water height of vent water column is slowly changed compared with the small vent area case. This is because of the capacity of the water column. So the pressure

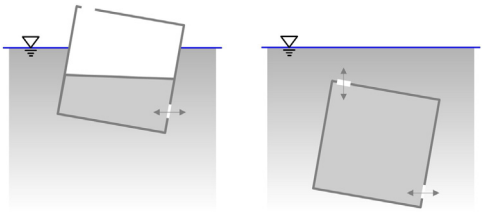

Fig. 13. Previous vented-compartment concept: floating (left) and submerged (right).

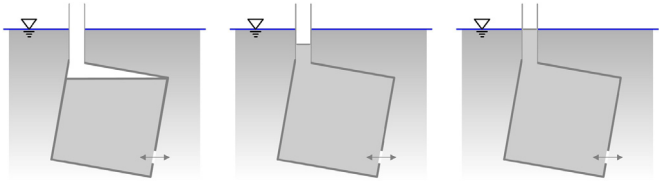

Fig. 14. Alternative vent air–water column concept for vented compartments.

fluctuation is expected to be larger for the small vent area case than for a large vent area. Verifying example will be appeared in Section 3.4.

3.3. Accumulator model

If a compartment is not vented, usually all the air does not flow out. Of course, all the air could flow out if there were any openings at the top of the compartment. If air remains in the compartment, the air pressure can be calculated using the state equation of air (Eq. (41)). On the other hand, if the amount of air is very small, the air pressure is so largely affected by the amount of water inflow, that it is difficult to calculate the air pressure. Furthermore, if all the air flows through an opening, there is no means to calculate the air density, thus a problem arises in calculating the reference pressure. In fact, a compartment in a ship might have machinery, freight, and many other things in it, so that there might be many small spaces that could contain air. This means that all the air in a compartment seldom flows out. Let us introduce a virtual accumulator that could solve this problem.

Fig. 15 shows the concept of a virtual accumulator for several cases: a case with remaining air, a case with a very small amount of remaining air, and a case without air. Air fills the accumulator, and its maximum volume is represented as V_{acmmax}, the operating volume is V_{acm}, and the air mass in the accumulator is m_{acm}.

A simple way to apply the accumulator is by adding the extra air volume without pre-charged pressure to the compartment volume, which cannot flow out. This is a passive accumulator.

$$
\begin{aligned}
&m_w = q_w \\
&m_a = q_a \ (for\ m_a \geq 0) \\
&V_w = m_w/\rho_w \\
&V_a + V_{acm} = V_{max} + V_{acmmax} - V_w \\
&\rho_a = \frac{m_a + m_{acm}}{V_a + V_{acm}} \\
&p_a = k_{atm}\rho_a^{\gamma} - p_{atm} \\
&V_a = m_a/\rho_a \\
&V_{acm} = m_{acm}/\rho_a
\end{aligned}
\tag{52}
$$

The virtual accumulator has the effect of enlargement of the volume. Even when there is no air the accumulator can provide a reference pressure and stabilize pressure fluctuation. If a passive accumulator is used, the mass conservation law is violated a little. However, if we want to conserve mass strictly, the active accumulator ensures it. An active accumulator makes the accumulator volume constant by controlling the amount of air. If the water flows in, the air in the accumulator is compressed so that the reference pressure rises and blocks the inflow of water. In this way, the active accumulator can give the reference pressure and ensures the mass conservation law in that compartment. A sudden inflow violates the mass conservation law, but in a short time, the appropriate amount of water flows out, so that the inner mass of compartment remains constant in reference to the concept of time average. The active accumulator model simply adds a feedback control law to regulate the volume of the accumulator. This allows the accumulator to maintain a nearly constant volume, and this feedback control changes the mass of the accumulator as in Eq. (53).

$$
\begin{aligned}
&V_{in} = V_{acmmax} - V_{acm} \\
&\dot{m}_{acm} = k_P V_{in} + k_D \dot{V}_{in}
\end{aligned}
\tag{53}
$$

where, k_P, k_D are the proportional and differential gains respectively, V_{in} means the change of the accumulator volume from its initial one (i.e., the volume that enters the accumulator).

For the maximum accumulator volume, we choose it in order that the enlargement of volume is less than 1% of the compartment volume, under the condition that the top position of a compartment is 2.5 m below the free surface. The resulting value is 5% of the compartment volume. Using this volume, the accumulator volume will be shrunk by an amount of 2.5% of the compartment total volume if the top of the compartment is 10 m below the free surface. This value of the accumulator volume always gave satisfactory results for the almost all the cases with a passive accumulator. About the gains of active accumulator, the proportional gain k_P is chosen so that the time constant (in the sense of the control theory) of the active control system is 1 second, and differential gain k_D is chosen to give a damping to this active accumulator system. The chosen values of the gains are $k_P = 1$ and $k_D \leq 5-10$ with $\Delta t = 0.01$ s. The author does not know this is the best choice, but it works well to fit the purpose of it.

3.4. Sample application

To view the effectiveness of the proposed compartment models, the sample calculations were carried out for the model geometry shown in Fig. 16.

The model in Fig. 16 has 4 compartments, and 5 openings. The Compartment 0 is fully vented, and others are non-vented compartments. The openings CID 0, 2, 3 are the ones connecting to outside, CID 1, 4 are for inside connection. The numbers appeared in Fig. 20 are dimensions in meter. The direction of arrows at the openings reveals the orientation of flow. The dimensions of openings CID 0, 2, 3 are (1 m × 1 m), (1 m × 1 m), (1 m × 0.5 m). CID 1 is a manhole which can show the down flooding, and it dimension is (0.5 m × 1 m). CID 4 is also a small manhole whose dimension is (0.5 m × 0.5 m). Compartment 1 has one opening in the ceiling: if flooding starts the compressed air blocks flooding, the water and air exchange can take place through the bubble forming. Compartment 2 has two openings up and down: the flooding process is easy and it will be fully-flooded at a short time. Compartment 3 has one side opening: the compressed air blocks the flooding after the inner water level reaches the top of opening. The Euler explicit method was chosen as a time integration scheme with a time step 0.02 s. And the model was fixed in space, in order to view the time behavior of flow well.

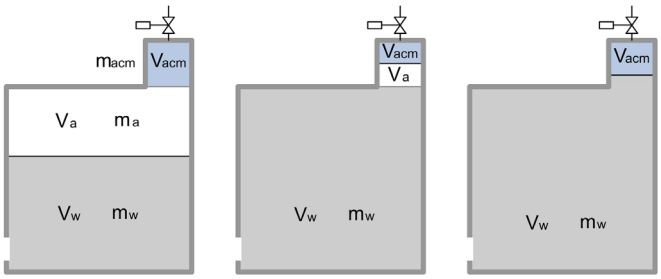

Fig. 15. Virtual Accumulator Model.

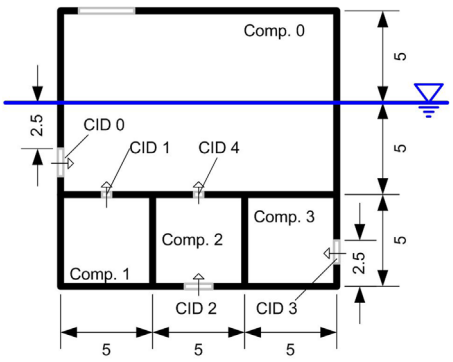

Fig. 16. Geometry for sample calculation of the compartment model.

The calculation was done under the condition of all non-vented compartment except Compartment 0.

Fig. 17 shows the filling ratios and air pressure in each compartment, and water flow through openings. The left figure shows the results with passive accumulator, and the right active accumulator. The main difference is the behavior of air pressure when the compartment becomes fully flooded. The model with active accumulator shows larger pressure fluctuation than with passive accumulator, while the active accumulator forces the filling ratio remains as 1 for fully flooded condition. For the flooding process of Compartment 1, the water flows freely from Compartment 0 in the early stage and the water level in Compartment 0 rises continuously. At about 7 s, the water in Compartment 0 blocks the opening CID 1, the water flows to Compartment 1 only if the pressure of water height is greater than the air pressure in Compartment 1. The air pressure rises up to the one of water height of Compartment 1, then the flow stops. After that, the water and air exchange takes place through bubble forming process, so the flow rate is low and the filling ratio rises slowly up to 1 as shown after 38 s in Fig. 17. For the flooding process of Compartment 2, in the early stage the water flows in through both openings CID 2 and 4. After about 7 s, the upper opening becomes blocked with the water so the air is compressed and flows out to Compartment 0. Around 16 s, the filling ratio reaches to 1, that is the air completely flows out, the pressure jumps up to high value. After that the water flows in through lower opening and the same amount of water flows out through upper opening until the water level in Compartment 0 reaches to its final value. In Compartment 3, the water flows in and air flows out through the opening CID 3 until the water level reaches to the top of the opening. After that moment, the compressed air blocks the water flow-in, and the pressure in Compartment 3 remains about the static pressure at the top of the opening.

In order to see the properties of vented compartment model, the calculations were carried out adopting the vented compartment model for Compartments 1 and 3. Fig. 18 shows the results; left figure shows the results with partially vented compartment with vent area 0.02 m^2, right figure shows the ones with fully vented compartment model. Using partially vented model, the air pressure rises as the filling ratio rises, the compressed air slows down the flooding process. Using fully vented model, the air pressure remains zero before the compartment is fully flooded, and the pressure jumps up to high value in order to balance the flows. The pressure fluctuation at the moment of fully flooding is larger in partially vented model than in fully vented model. This is because that the area of water column in vent duct is small in partially vented model, so that flow through openings can make the up and down movement easily. Addition to this, the change of

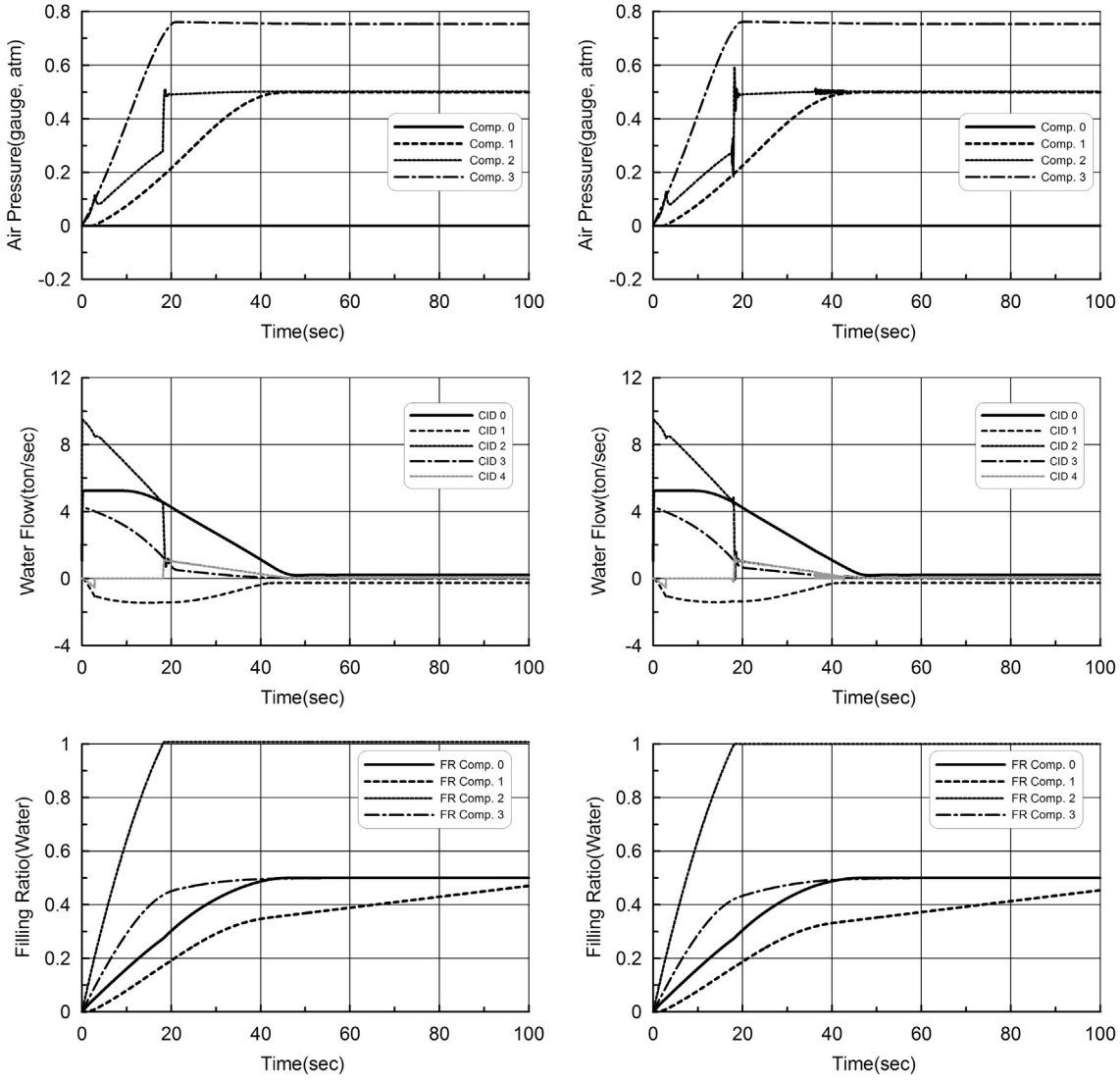

Fig. 17. Time simulation results for the model in Fig. 16 (Compartment 0-fully vented, Compartment 1,2,3-non-vented), left–passive accumulator, right–active accumulator.

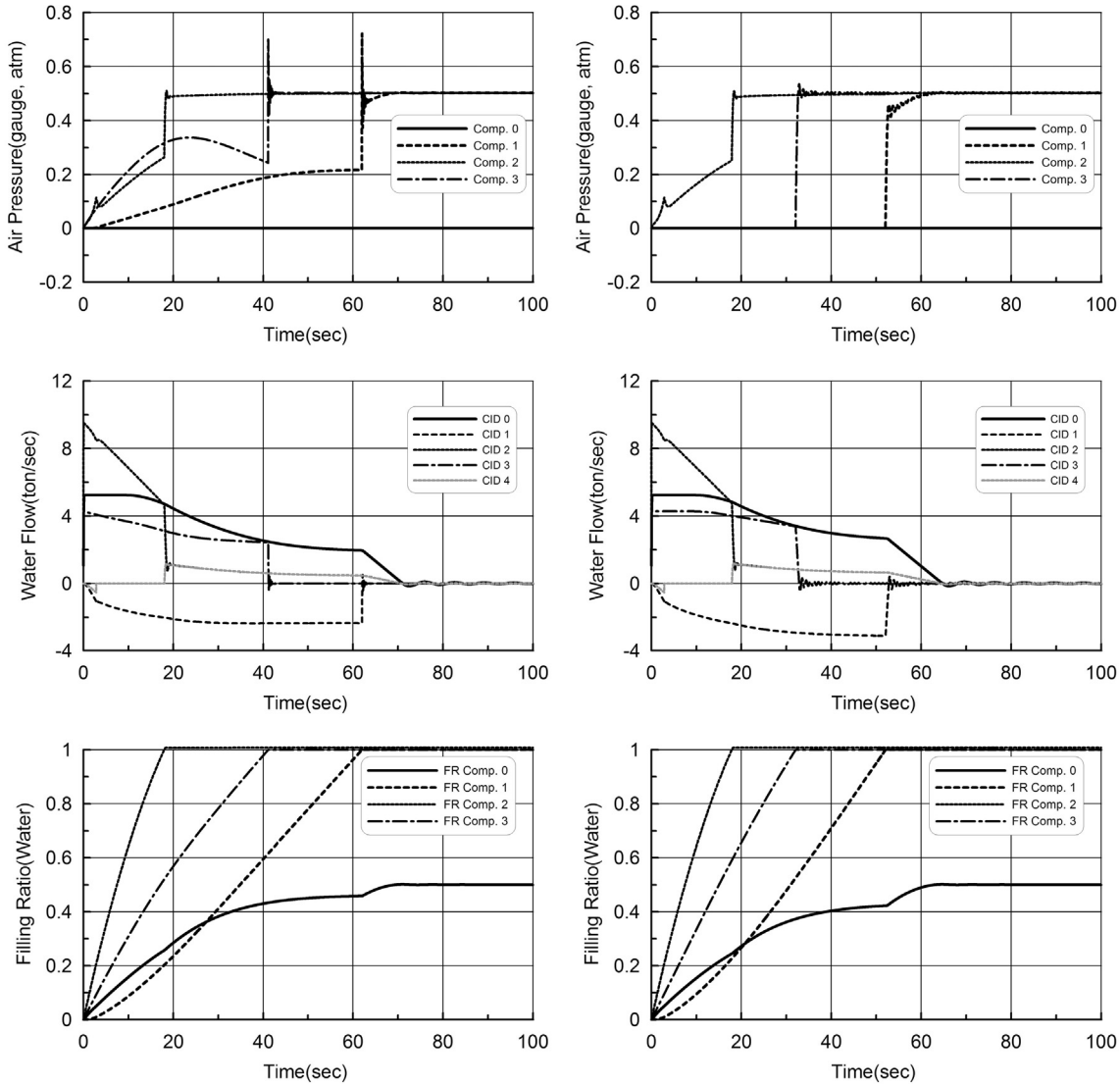

Fig. 18. Time simulation results for the model in Fig. 16 (Compartment 0-fully vented, Compartment 2-non-vented), Compartment 1,3: left-partially vented with vent area 0.02 m^2, right-fully vented.

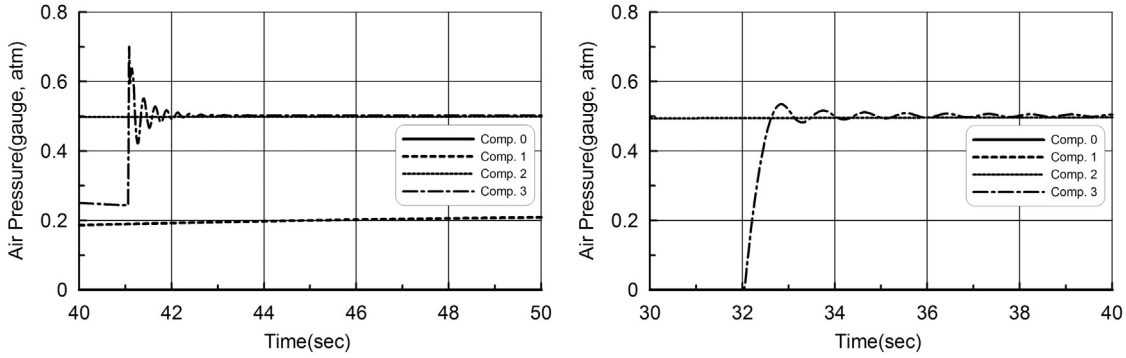

Fig. 19. Enlarged view of the air pressure fluctuation around the moment of fully filled in Compartment 3. (left-partially vented with vent area 0.02 m^2, right-fully vented).

flow material through the vent from air to water makes the pressure jump-up, and the small area makes this jump-up large. The slow pressure change to the final value after 53 s in Compartment 1 is due to the water level in Compartment 0 for fully vented case. Fig. 19 shows the pressure fluctuation. For a partial vent model, the pressure fluctuates more and the period is shorter than for a full vent model.

The above sample applications show well the properties of down flooding, trapped air, vent, and fully flooded compartment, and give the verification of the compartment model proposed in this section.

4. Application

This section is added to show how the previous models had been used, and what example they applied to.

4.1. Flooding simulation program

In order to simulate the flooding and sinking of a real ship, a number of modeling and calculation techniques other than previously stated models are required. Let us list them up based on KRISO's own simulation program SMTP.

4.1.1. Compartment geometry model

What needed with the inner compartment for flooding simulation are the center of gravity, and the water height from its lowest point for any given volume of water in it and for any inclination angle (roll and pitch). A 3-dimensional model of a compartment is the best, but the above mentioned quantities are hard to calculate with general 3-D model. Therefore a cylindrical shaped geometrical model whose fore and aft sectional shapes are different to each other and have polygonal shapes should be prepared. At least, the compartment geometry should be a cylindrical shaped geometry with one polygonal section. And it is needed to calculate the pressures at the openings or at the corner points of opening for any angle of inclination.

4.1.2. Compartment flow model

A tool should be provided to calculate the mass flow through openings. The pressures at both sides of opening are provided by the compartment geometry model. The model of Section 2 would be used for this purpose.

4.1.3. Pipe and duct model

Almost all the compartments are connected to adjacent ones by at least one general opening (door, hatch) but some compartments are also connected to others by pipes or ducts. Moreover, a few compartments have pipes whose outlets connect with the outside (bilge pipe). And for air vents, the vent inlet is located over the main deck. These examples have the property that the opening inlet is apart from the corresponding compartment. There need a tool to calculate the flow through pipe or duct provided with the pressures at both ends. And it should count on the pressure drop due to the length of pipe and the effect of various fittings.

4.1.4. Down flooding model

In compartments with an opening at the bottom, the water flows down freely if the compressibility of air is neglected. If the compressibility of air is taken into account, and there is no other opening at the top, the negative pressure blocks the downward flow of water. For another case, a compartment with an opening on top covered by water, the compressed air blocks the inflow of water. However, for a large opening, the exchange of water and air takes place with the process of bubble forming. Even though its flow rate is small, it is required for the compartment located at the bottom of a ship.

4.1.5. Floodwater dynamics model

The floodwater in a compartment moves due to the motion of a ship. And the movement of floodwater affects the ship motion. The main parameter of this effect is the center of gravity of floodwater. It is required to calculate the movement of the center of gravity of floodwater due to the ship motion considering the dynamics of floodwater, while it has simple dynamics.

4.1.6. 6-DOF ship motion program

The above all models should be imported into a ship motion program. Floodwater has effect to ship motion by changing the total mass of the ship and its center of gravity. The ship motion program had better to have 6-DOF(degree of freedom). At least 3-DOF (heave, pitch, roll) should be solved in order to simulate the flooding and sinking of a ship. The buoyancy force and moment should be calculated without assumption of linearity, for all range of roll angle (from negative 180° to 180°), and even under the condition of deck submergence. The other forces acting on the ship may be used as in a conventional ship motion program, including radiation forces (in the form of impulse response functions) and wave exciting forces in order to analyze the capsize rate and time for a damaged ship in irregular waves.

4.2. Application example

Recently, there was a sinking accident with the loss of many people in Korea. The ship, MV Sewol, was a Ro-Ro ferry of 132 m length, 22 m breath, and 9610 ton displacement. It has two car decks and a freight deck in it. After this accident, there were many hypotheses about the cause of it, some scientific and some groundless. It was required to prepare the scientific explanation of this accident. The simulation team in KRISO was launched in order to make data to reasonably explain the cause and effect of the accident

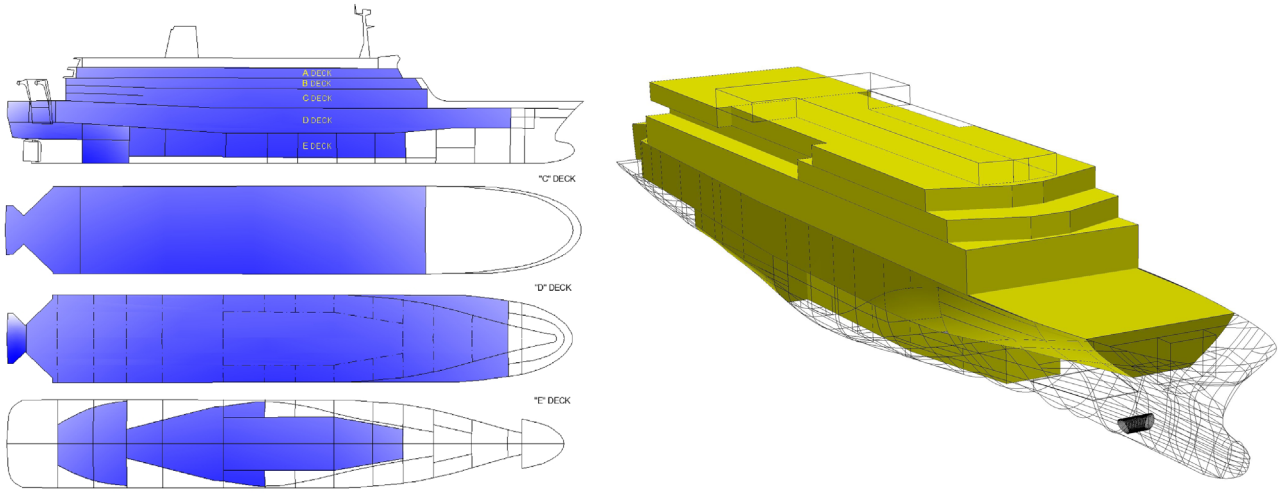

Fig. 20. Shape and the internal compartment of MV Sewol.

(KRISO, 2014). The data prepared were GA (general arrangement), design drawings and booklets, loading table and drafts at departure, track record of the ship, and the inclination angles with time stamp after the coast guard arrived(these angles was drawn by the expert from pictures taken by the coast guard, and accepted as official data by the cooperative investigation headquarter). The data during accident were not enough. The simulation team consisted of two subteams. One was for the analysis of the maneuvering behavior and the other one was for flooding and sinking. The main reason of the accident turned out to be the lack of restoring and the movement of freight during its turn.

Let us briefly introduce the work of flooding simulation team. They used KRISO's own simulation program which can simulate the ship motion of 6-DOF in time domain including flooding process mentioned in previous sections, in which the time integration scheme was Euler explicit method with time step 0.02 s. The ship was modeled with 27 internal compartments and 81 openings for flooding simulation. The all compartments below the main deck which can be flooded were modeled except the fuel, fresh water, and ballast tanks. Two car decks were modeled, which were so simple to model. The living quarters (passenger decks, A, B) had too many rooms to model it, so the each passenger deck was simplified and modeled with 4–5 compartments. Fig. 20 shows the shape of the ship and compartments in it. The flooding simulation team had tried to tune up the parameters (especially related with openings, the gap of doors and ramps) so in order that the simulation results resemble the official data from the cooperative investigation headquarter for MV Sewol. Then, the team provided explanations about the process of the flooding and sinking.

It was presumed that the ship tumbled down due to an excessive steering and the resulting movement of freight in it. It was reported the initial angle of heel was 30° port after its tumble and there was no collision accident, and the wave height was very low. The flooding simulation started from the condition in which the roll angle was negative 30° (i.e., the left side of the ship went down). Fig. 21 shows the roll angle (inclination) compared with the official data provided by the cooperative investigation headquarter for MV Sewol. Figs. 22 and 23 show the pitch and heave motion during flooding and sinking.

Fig. 23 shows the flow rate through some important openings from outside. And Fig. 24 shows the filling ratios in compartments below the main deck. At the start, the flow-in took place only through the side door located at D deck, which was 3.5 m high from the sea level when upright condition. As the inclination went larger, the flow-in through the stern ramps began to grow. There were only 3 openings through which the sea water flows in before 2700 s. The resulting floodwater was accumulated on D deck and E deck (these decks is located under the main deck). After 2700 s, the sea water flowed in through the vent of the left stabilizer room. And thereafter, many other compartments flooded.

The side door located at D deck and the rear ramps are assumed to be closed. The simulation team assumed gap of 0.01 m along the edge of the door and ramps. It could be said that the only 0.01 m of gap size of a side door and rear car ramp are sufficient to flooding and sinking of Ro-Ro ferry.

Fig. 25 shows the important situations to be noticed: initial condition of flooding simulation, the ship when coast guard arrived, when the last rescue action played, finally capsized. The results reflect the actual situations well, in comparison with the pictures that have shown in many mass media.

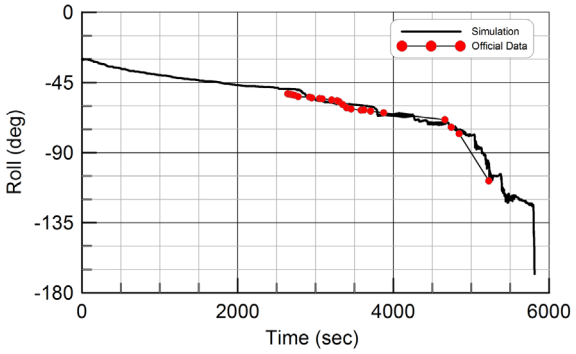

Fig. 21. Simulated inclination angle(roll) compared with the official data during the flooding and sinking process. (The official data were drawn by the expert from pictures taken by the coast guard, and accepted by the cooperative investigation headquarter).

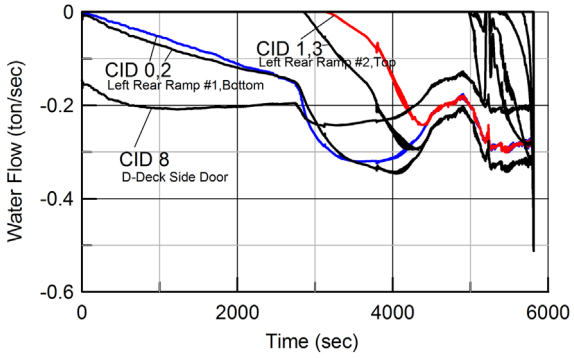

Fig. 23. Flow rate of water through important openings.

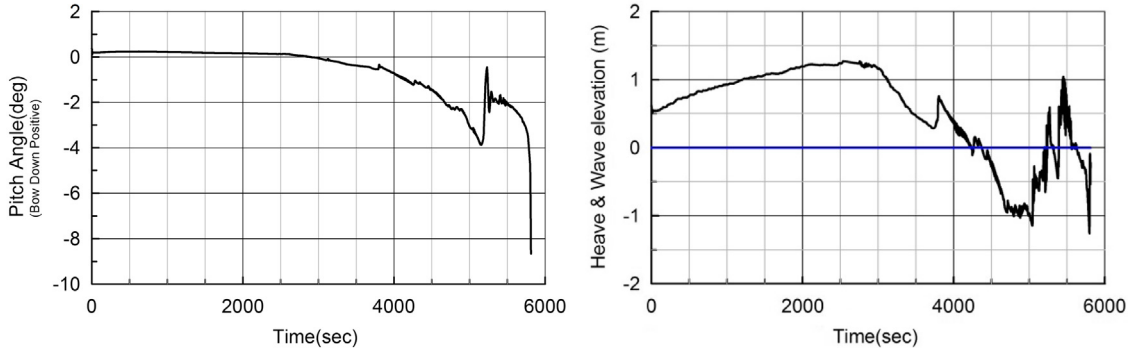

Fig. 22. Simulated pitch(left) and heave(right) during the flooding and sinking process.

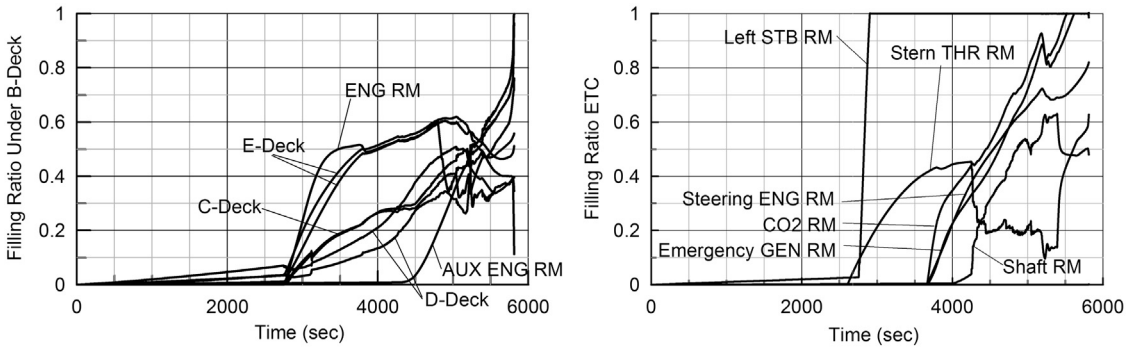

Fig. 24. Filling ratios of the lower compartments (below main deck).

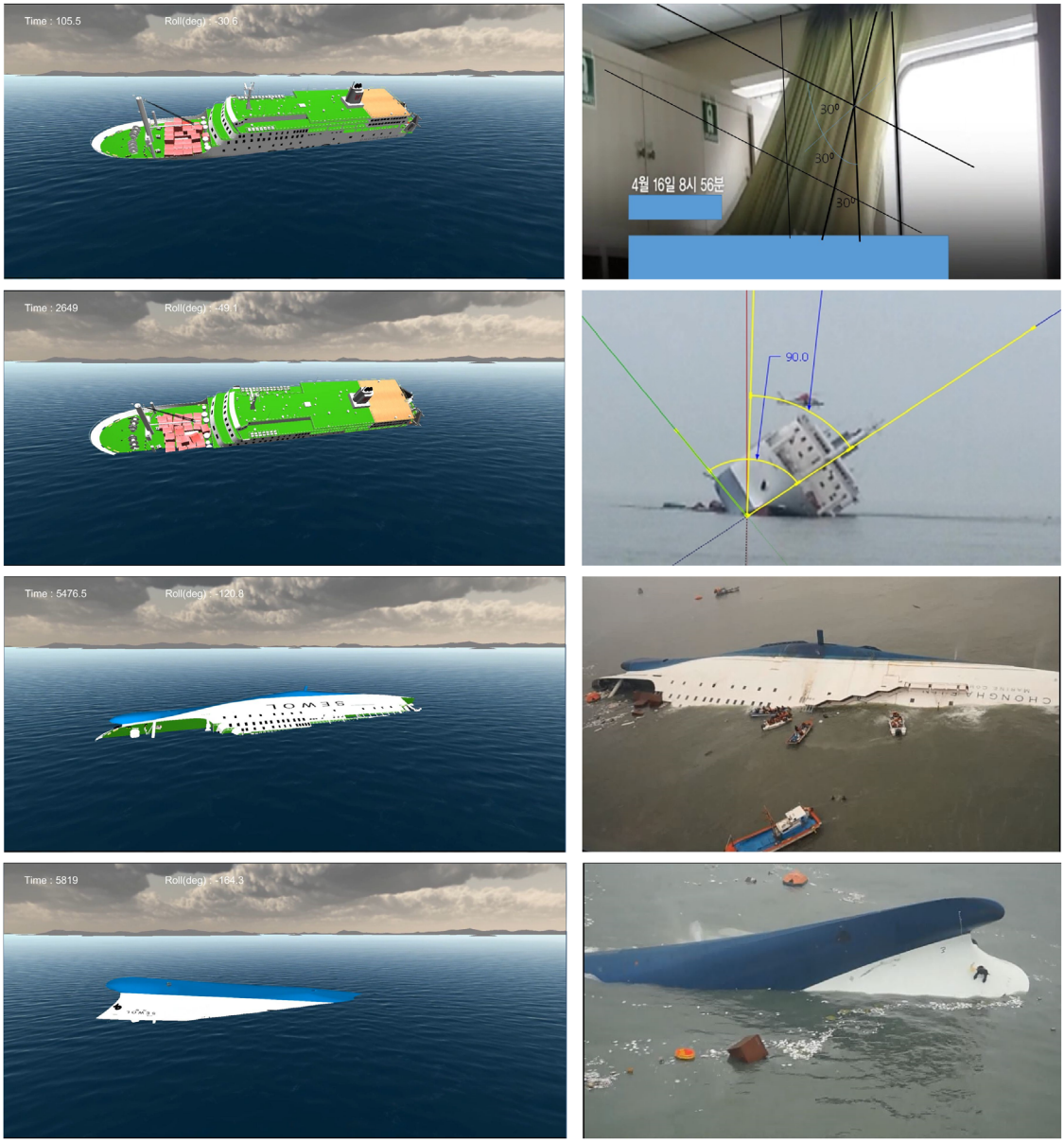

Fig. 25. Visualizations of the simulation results and the real situations(1st set: initial state, 2nd set: when the coast guard arrived, 3rd set: right after the last rescue action ended, 4th set: final state, There is no picture taken from outside at the initial state).

5. Conclusions

In this study, flow models for simulation of ship flooding were investigated. The most important matters were the orifice equations and the compartment models.

For the orifice equation, it was shown that numerical instability could occur involving the air flow, if the hydraulic orifice equation is used to calculate the flow through an opening. A newly derived dynamic orifice equation by Lee (2014) was investigated that could resolve the numerical instability that comes from the square root of the pressure difference. For verification, a number of sample calculations were carried out. From these, our findings are: a point opening should not be used for the case of only one opening in a compartment; a dynamic orifice equation has its ability to resolve the numerical instability especially for small pressure difference.

A new compartment model that can provide pressure balance automatically was proposed. It reduces the computational burden and difficulty in applying the pressure-correction method. It includes vented and non-vented compartment model for a fully-flooded compartment which has difficulty in determining a reference pressure. It also includes an accumulator model which can damp out the excessive pressure fluctuation when the compartment is nearly full-filled, and can give the reference pressure even for a fully-flooded. From verification calculations, the proposed model turns out to work well for various situations such as, down flooding, vented and non-vented compartment, and fully filled condition.

This paper dealt with modeling for flooding simulation, and the focus was on the modeling itself and verification. The validation study should be followed by comparing the simulation results with an appropriate model test data (probably from Ruponen, 2007).

As an application example of these models, the brief of flooding simulation of a recent actual accident were introduced. The simulation using the above models gave the reasonable results about the cause and effect of that accident. And the process of flooding and sinking could be explained approximately, but reasonably, when the results were compared with official data.

Acknowledgment

In the accident mentioned in this study, the ship sank with the loss of many people, dead or missing. The data included in Section 4 are parts of the report of the simulation team for the accident of Ro-Ro ferry. The writer feels sorry for not adding the details of the report of the simulation team of this accident in this paper. The writer hopes that this study helps to make ships safer. This study was partially supported through a basic project of KRISO(PES1990).

Appendix A. Derivation of the proposed dynamic orifice equation

(This part, Appendix A, is a translation of a part of Lee (2014), which is written in Korean.)

Let us assume that the fluid is incompressible and inviscid. The definitions of variables and geometry related in this derivation can be found in the explanation of Eqs. (6), (6′), (7) and (7′) and Fig. 2 in the Section 2.2.

The integral version of the mass and momentum conservation law can be represented by the following, for a specific control volume.

$$\int_{\partial\Omega}\rho\left(\vec{v}.\vec{n}\right)dS=0 \qquad (A-1)$$

$$\int_{\Omega}\frac{\partial}{\partial t}\left(\rho\vec{v}\right)dV+\int_{\partial\Omega}\rho\vec{v}\left(\vec{v}\cdot\vec{n}\right)dS=\int_{\Omega}\rho\vec{F}dV-\int_{\partial\Omega}p\vec{n}dS \qquad (7)$$

$$\int_{\Omega}\frac{\partial}{\partial t}\left(\rho\vec{v}\right)dV+\frac{1}{2}\int_{\partial\Omega}\rho\left(\vec{v}\cdot\vec{v}\right)\vec{n}dS=\int_{\Omega}\rho\vec{F}dV-\int_{\partial\Omega}p\vec{n}dS \qquad (7')$$

The velocity components excluding u are asymmetric about the centerline of the orifice. Let us apply the Eqs (A-1), (7) and (7′) to the control volumes C_0 and C_1.

Control volume C_1

If we apply the continuity Eq. (A-1) for C_1,

$$u_1A_1=\int_{A_1}u\,dA=Q \qquad (A-2)$$

where, Q is the volumetric flux through an orifice, the Euler equation becomes

$$\vec{i}\int_{\Omega}\frac{\partial}{\partial t}(\rho u)dV=-\vec{i}\int_{\partial\Omega}(p_1-p)\,dS \qquad (A-3)$$

$$\therefore\ \int_A pdA=A_1p_1+\int_{C_1}\frac{\partial}{\partial t}(\rho u)dV \qquad (A-4)$$

Control volume C_0

On C_0, the continuity equation becomes

$$v_n2\pi R^2+\int_{A_1}u\,dA=0$$

$$v_n=-\frac{1}{2\pi R^2}\int_{A_1}u\,dA=-\frac{1}{2\pi R^2}Q \qquad (A-5)$$

Let us represent this velocity in vector form as

$$\vec{v}=-\vec{n}\frac{1}{2\pi R^2}Q\quad on\ A_R \qquad (A-6)$$

Apply the momentum conservation Eq. (7) for C_0, then

$$\int_{C_0}\frac{\partial}{\partial t}(\rho u)dV+\int_{\partial\Omega}\rho u\left(\vec{v}\cdot\vec{n}\right)dS=-\int_{\partial\Omega}pn_xdS \qquad (A-7)$$

The second integral of the above equation can have a value on A and A_R. However, the integral over A_R behaves like R^{-2}, so the integral vanishes as R gets large enough. The integral on the right side, the pressure integral, can be represented as

$$\int_{\partial\Omega}pn_xdS=-\int_A(p_0-p)dA-\int_{A_0-A}(p_0-p)dA \qquad (A-8)$$

(from $\int_{A_R}pn_xdS=p_0\int_{A_R}n_xdA=p_0\int_{A_0}dA=\int_{A_0}p_0dA$)

The last integral of Eq. (A-8) is the one over the wall, and the pressure on the wall is slightly less than p_0. The pressure goes to p_0 because the distance from the orifice center is large, and near the orifice, the pressure is that of the orifice. Therefore, the second integral on the right side of the equation is positive, and is less than the first integral in the right side. Let us represent this as δF_p. The momentum conservation law (A-7) becomes

$$\int_{C_0}\frac{\partial}{\partial t}(\rho u)dV+\int_A\rho u\cdot udA=\int_A(p_0-p)dA+\delta F_p \qquad (A-9)$$

Substituting Eq. (A-4) into the right side of the equation above (A-9), and defining the average normal velocity square as $\int_A u\cdot ud A=\overline{u^2}A$ gives

$$\int_{C_0}\frac{\partial}{\partial t}(\rho u)dV+\int_{C_1}\frac{\partial}{\partial t}(\rho u)dV+\rho\overline{u^2}A=(p_0-p_1)A+\delta F_p \qquad (A-10)$$

Where an over bar means the average.

Since the fluid is assumed to be incompressible and inviscid, the velocity field can be represented by the velocity potential. Therefore the pressure on the wall can be represented as follows using the velocity potential and the Bernoulli equation.

$$\delta F_p=\int_{A_0-A}(p_0-p)dA=\rho\int_{A_0-A}\left(\phi_t+\frac{1}{2}V^2\right)dA$$

$$= \rho \int_{A_0-A} \phi_t dA + \rho \frac{1}{2} \int_{A_0-A} V^2 dA$$

Substituting this equation into (A-10) gives

$$\int_{C_0} \frac{\partial}{\partial t}(\rho u) dV + \int_{C_1} \frac{\partial}{\partial t}(\rho u) dV - \rho \int_{A_0-A} \phi_t dA + \rho \overline{u^2} A - \frac{1}{2} \rho \int_{A_0-A} V^2 dA = (p_0 - p_1) A \quad (A-11)$$

Now, let us apply the second equation of momentum conservation (7′) for C_0. In line with the similar procedure from (A-7)–(A-11), we get the following momentum equation.

$$\int_{C_0} \frac{\partial}{\partial t}(\rho u) dV + \int_{C_1} \frac{\partial}{\partial t}(\rho u) dV - \rho \int_{A_0-A} \phi_t dA + \frac{1}{2} \rho \int_{A_0-A} V^2 dA = (p_0 - p_1) A \quad (A-12)$$

The Eqs. (A-12) and (A-11) are the same; in fact, the only difference is in their expression.

Let us introduce the concept of added mass in order to simplify the equations. The first three terms of Eqs. (A-11) and (A-12) are related to the added mass. If the fluid is inviscid and there is no free surface, the total flow varies instantly when the velocity at the orifice changes. This flow is independent of time, and proportional to the orifice velocity. Therefore, the following expression can be used.

$$\int_{C_0} \frac{\partial}{\partial t}(\rho u) dV = m_{C_0} \frac{\partial u_{open}}{\partial t}, \quad \int_{C_1} \frac{\partial}{\partial t}(\rho u) dV = m_{C_1} \frac{\partial u_{open}}{\partial t}$$

$$m_{C_0} = \rho \int_{C_0} \frac{u}{u_{open}} dV, \quad m_{C_1} = \rho \int_{C_1} \frac{u}{u_{open}} dV,$$

$$m_\phi = -\rho \int_{A_0-A} \phi_t / u_{open} dV \quad (A-13)$$

Take the average velocity as the representative velocity, as in the following equation.

$$\overline{u} = \frac{1}{A} \int_A u dA \quad (A-14)$$

On the wall, $A_0 - A$, the velocity square can be represented as

$$V^2 = \frac{1}{\left(2\pi R^2\right)^2} (\overline{u})^2 A^2 = \left(\frac{A}{2\pi R^2}\right)^2 (\overline{u})^2 \quad (A-15)$$

Then, the integral over $A_0 - A$ of Eq. (A-11) becomes

$$I = \frac{1}{2} \int_{A_0-A} V^2 dS = \frac{1}{2} \int_{R_0}^{\infty} \left(\frac{A}{2\pi R^2}\right)^2 (\overline{u})^2 2\pi R \, dR = \frac{1}{2} (\overline{u})^2 \frac{A^2}{2\pi} \int_{R_0}^{\infty} \frac{1}{R^3} dR = \frac{1}{2} (\overline{u})^2 \frac{A^2}{2\pi} \frac{1}{2R_0^2} \quad (A-16)$$

If we take R_0 as the radius of orifice, that is $A/(\pi R_0^2) = 1 \rightarrow R_0^2 = A/\pi$, then Eq. (A-16) is reduced to the simple expression.

$$I = \frac{1}{2} (\overline{u})^2 \frac{A^2}{2\pi} \frac{1}{2R_0^2} = \frac{1}{8} (\overline{u})^2 A \quad (A-17)$$

Applying Eqs. (A-13) and (A-17) for the momentum conservation law, and using the average velocity, Eqs. (A-11) and (A-12) can be written as

$$m_a \frac{\partial \overline{u}}{\partial t} + \rho \overline{u^2} A - \frac{1}{8} \rho (\overline{u})^2 A = (p_0 - p_1) A \quad (A-18)$$

$$m_a \frac{\partial \overline{u}}{\partial t} + \frac{1}{2} \rho \overline{V^2} A = (p_0 - p_1) A \quad (A-19)$$

where, $m_a = (m_{C_0} + m_{C_1} + m_\phi)$. The average of the velocity square and the square of the average velocity might be slightly different, but if we assume that this difference is small enough that these two are the same, then the Eqs. (A-18) and (A-19) become

$$m_a \frac{\partial \overline{u}}{\partial t} + \frac{7}{8} \rho (\overline{u})^2 A = (p_0 - p_1) A \quad (A-20)$$

$$m_a \frac{\partial \overline{u}}{\partial t} + \frac{1}{2} \rho (\overline{V})^2 A = (p_0 - p_1) A \quad (A-21)$$

Since the above two equations are the same, we can obtain the following relationship.

$$\frac{7}{8} (\overline{u})^2 = \frac{1}{2} (\overline{V})^2 \rightarrow (\overline{u})^2 = \frac{4}{7} (\overline{V})^2 \quad (A-22)$$

This shows that the contraction coefficient for a circular orifice with a right-angle edge is theoretically $\sqrt{4/7} \cong 0.756$. (Of course, this is for an invicid fluid.)

Added mass m_a in the Eqs. (A-20) and (A-21) means the amount of surrounding fluid that moves proportionally with the velocity at orifice. We use that of a circular disk as m_a in the equations, $m_a = 8/3 \, \rho r^3$(Lamb, 1945), where r is the radius of circular disk, so take $r = \sqrt{A/\pi}$.

$$m_a = \frac{8}{3\pi} \rho A \sqrt{A/\pi} = \frac{8}{3\pi^{3/2}} \rho A \sqrt{A} \quad (A-23)$$

For our problem, the wall might have an effect to block the flow, so the added mass seems to be slightly larger than this value. According to this reasoning, the coefficient in the above equation $8/(3\pi^{3/2})$ may be approximated by 1/2.

$$\frac{\sqrt{A}}{2} \frac{\partial \overline{u}}{\partial t} + \frac{7}{8} (\overline{u})^2 = \frac{(p_0 - p_1)}{\rho} \quad (A-24)$$

$$\frac{\sqrt{A}}{2} \frac{\partial \overline{u}}{\partial t} + \frac{1}{2} (\overline{V})^2 = \frac{(p_0 - p_1)}{\rho} \quad (A-25)$$

The above two equations are the same, and are applicable for $\overline{u} > 0$. Of the two equations, it is more convenient to use Eq. (A-24) because it uses the velocity normal to the orifice, not the total velocity.

Appendix B. Square root instability

The hydraulic orifice equation was originally for steady state, let us see what happens if we apply it for an unsteady case. Here, the point of focus is the fact that the flow velocity is represented using the square root of the pressure difference. The square root function presents no problem for a large argument, but for small arguments, there is an issue. The differential of the square root function does not exist for zero pressure difference. Thus, it is impossible to expand with a Taylor series about zero. Consider the situation in Fig. B-1, in which both sides are filled with air, and there is an opening between them. The final state is the one in which the pressures on both sides are the same, so the pressure difference is zero.

Let us formulate the above situation. The mass flow could be represented as

$$q = sgn(\Delta p) \rho A \sqrt{\frac{2|\Delta p|}{\rho}} = sgn(\Delta p) A \sqrt{2\rho} \sqrt{|\Delta p|} \quad (B-1)$$

The air masses in both compartments would change according to

$$\dot{m}_{a0} = -q$$
$$\dot{m}_{a1} = q \quad (B-2)$$

The pressure in each compartment can be determined under the assumption of iso-entropic process of air. (γ is the specific heat,

7/5 for an iso-entropic process, and 1 for an iso-thermal process)

$$p_0 = k_a\rho_0^\gamma - p_{atm} = k_a\left(\frac{m_{a0}}{V_0}\right)^\gamma - p_{atm}$$
$$p_1 = k_a\rho_1^\gamma - p_{atm} = k_a\left(\frac{m_{a1}}{V_1}\right)^\gamma - p_{atm} \quad (B-3)$$

$$k_a = p_{atm}/\rho_{atm}^\gamma.$$

Take the time differentiation of the above equations, and substitute Eq. (B-2) in them,

$$\dot{p}_0 = \gamma\frac{k_a}{V_0}(m_{a0})^{\gamma-1}\dot{m}_{a0} = -\gamma\frac{k_a}{V_0}(m_{a0})^{\gamma-1}q$$
$$\dot{p}_1 = \gamma\frac{k_a}{V_1}(m_{a1})^{\gamma-1}\dot{m}_{a1} = \gamma\frac{k_a}{V_1}(m_{a1})^{\gamma-1}q \quad (B-4)$$

Here, we assume the same volume of compartments (i.e., $V_0 = V_1$). If the pressures are the same initially, then air masses in both compartments are the same initially. Assume the change of air masses is small, and the mass could be assumed as constant m_a for the last expression of Eq. (B-4). If the flow through an opening increases the pressure of one compartment, the pressure of the other compartment goes down, so that $p_1 = -p_0$. The atmospheric pressure is large enough so that the density is nearly constant, so Eq. (B-4) can be rewritten as, after substituting Eq. (B-1),

$$\dot{p}_0 = -\gamma\frac{k_a}{V}(m_a)^{\gamma-1}sgn(p_0)2A\sqrt{\rho_{atm}}\sqrt{|p_0|}$$
$$= -2\gamma\frac{A}{V^{2-\gamma}}\frac{p_{atm}}{\sqrt{\rho_{atm}}}sgn(p_0)\sqrt{|p_0|} \quad (B-5)$$

Let us rewrite this into a simpler form.

$$\dot{p} = -Ksgn(p)\sqrt{|p|} \quad (B-6)$$

where $K = 2\gamma\frac{A}{V^{2-\gamma}}\frac{p_{atm}}{\sqrt{\rho_{atm}}}$

The value of K is very large. One solution of the above equation is $p = 0$, which is what we want. Let us examine the numerical solution, using the Euler method,

$$p^{n+1} = p^n - Ksgn(p)\sqrt{|p^n|}\Delta t \quad (B-7)$$

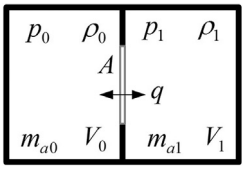

Fig. B-1. Arrangement of the sample problem.

We know the pressure would bounce around zero, because of the large value of K. Let us seek the amplitude of oscillation p^*.

$$-p^* = p^* - K\sqrt{p^*}\Delta t \rightarrow \therefore\ p^* = 0 \text{ or } p^* = \frac{(K\Delta t)^2}{4} \quad (B-8)$$

The oscillating solution is as follows.

$$p^n = (-1)^n(K\Delta t)^2/4 \quad (B-9)$$

No matter what the absolute value of the pressure was initially, the amplitude of pressure oscillation converges to p^*. That is a type of self-sustained oscillation (or self-excited). Even though we use the predictor-corrector, or Runge-Kutta method, the pressure will not go to zero, and does not oscillate as in Fig. B-2.

The above figure shows that even if the initial value is infinitesimally small (not zero) or larger than p^*, the result of the Euler method oscillates back and forth around zero and the amplitude grows to p^*. However, the results of the predictor-corrector do not oscillate and go to the value of p^*. Even for the Runge–Kutta method, it goes to about $1/4\ p^*$, not zero. This is numerically unstable. Because the predictor-corrector and Runge–Kutta methods give non-zero solutions, they are dangerous compared with the Euler method. The result of the Euler method gives values whose average is zero. We expected the solution to go to zero, but it does not, so this phenomenon can be called numerical instability.

Let us investigate the value of K,

$$K = 2\gamma\frac{A}{V^{2-\gamma}}\frac{p_{atm}}{\sqrt{\rho_{atm}}}$$

Substitute the real values except A and $V(\rho_{atm} = 1.26, p_{atm} \cong 100,000)$

$$K = 178,174 \times \gamma\frac{A}{V^{2-\gamma}} = 356,348 \times \frac{A}{V^{0.6}} \quad (B-10)$$

In order to maintain p^* as less than 100 Pa (i.e., 1/1000 of atmospheric pressure; this would be accepted as a negligible amount in the engineering sense) the time interval of simulation should be the following value.

$$\Delta t^* = 20/K = 5.6 \times 10^{-6}\frac{V^{0.6}}{A}$$

For example, a passenger ship has many rooms in which the dimensions are about 4 m(depth), 3 m(width), and 2.5 m(height), for which the area of door is 2 m^2, and for that room $\Delta t = 0.00022$. This is not practical. For a larger compartment of 10 m × 10 m × 5 m, with a 2 m^2 door, the time interval should be $\Delta t = 0.001$. Therefore, this is impractical because of the numerical instability of the square root.

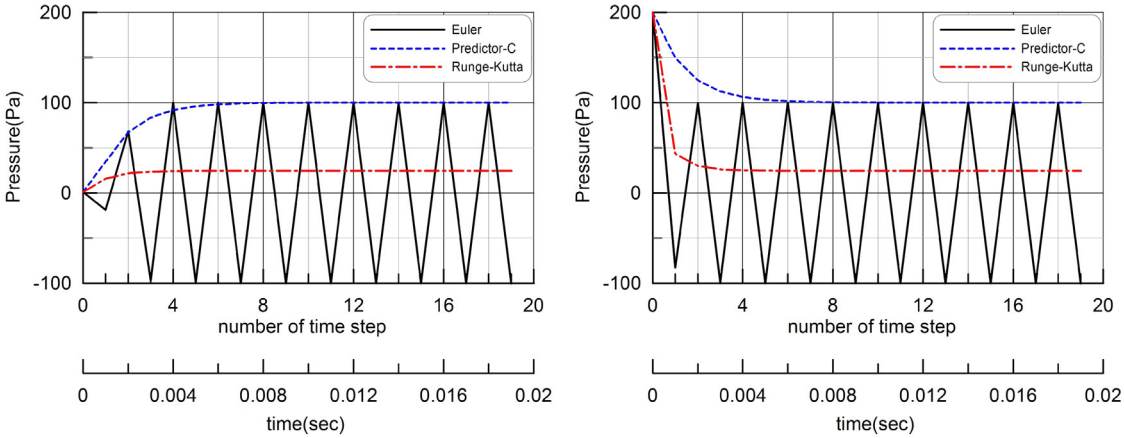

Fig. B-2. Numerical solution of the air pressure revealing the square root instability. (K=20,000, Δt=0.001, p^*=100).

References

Chang, B.-C., Blume, P., 1998. Survivability of damaged ro-ro passenger vessels. Schiffstechnik – Ship Technol. Res. 45, 105–112.

Chang, B.-C., 1999. On the damage survivability of Ro-Ro ships investigated by motion simulation in a seaway. Schiffstechnik – Ship Technol. Res. 46, 192–207.

Cho, S. K., Hong, S. Y., Kim, Y. H., and Lee, K. J., 2005. Investigation of dynamic characteristics of the flooding water of the damaged compartment of an ITTC RORO Passenger Ship, In: Proceedings of the 8th International Ship Stability Workshop, Istanbul, Turkey, 6–7 October 2005.

Dankowski, H., 2013. A Fast and Explicit Method for Simulating Flooding and Sinkage Scenarios of Ships (Doctoral dissertation). Technical University of Hamburg-Harburg, Hamburg, Germany.

Ikeda, Y., Ishida, S., Katayama, T., and Takeuchi, Y., 2004. Experimental and Numerical Studies on Roll Motion of a Damaged Large Passenger Ship in Intermediate Stages of Flooding, In: Proceedings of the 7th International Ship Stability Workshop, Shanghai, China, 1–3 November 2004, pp. 42–46.

KRISO, 2014. Analysis of the cause of a sinking accident of MV Sewol (Simulation of Maneuvering, Flooding, and Sinking). KRISO, Korea, pp. 114–129, Report No. UCPGS2750-10546-6.

Lamb, H., 1945. Hydrodynamics. Dover Publications, Inc., New York, p. 164 (republication of the 6th(1932) edition by Cambridge University Press).

Lee, G. J., 2010. Simplified modelling of floodwater dynamics, In: Proceedings of the Annual Autumn Meeting, SNAK, Changwon, 21–22 October 2010, pp.969–974. (in Korean).

Lee, G.J., 2014. A study on the dynamic orifice equation for the flooding simulation of a ship. J. Ships Ocean Eng. 55, 17–27.

Palazzi, L., de Kat, J., 2004. Model experiments and simulations of a damaged ship with air flow taken into account. Mar. Technol. 41, 38–44.

Papanikolaou, A., Zaraphonitis, G., Spanos, D., Boulougouris, E., and Eliopoulou, E., 2000. Investigation into the capsizing of damaged Ro-Ro Passenger Ships in waves, In: Proceedings of the 7th International Conference on Stability of Ships and Ocean Vehicles, Launceston, Tasmania, Australia, 7–11. February 2000, pp. 351–362.

Ruponen, P., 2006. Pressure-correction method for simulation of progressive flooding and internal air flows. Ship Technol. Res. – Schiffstechnik 53, 63–73.

Ruponen, P., 2007. Progressive flooding of a damaged passenger ship (Doctoral dissertation). Helsinki University of Technology, Finland.

Ruponen, P., Kurvinen, P., Saisto, I., Harras, J., 2013. Air compression in a flooded tank of a damaged ship. Ocean Eng. 57, 64–71.

Spouge, J.R., 1986. The technical investigation of the sinking of the Ro-Ro Ferry European gateway. Trans. R. Inst. Naval Arch. 128, 49–72.

Sen, P., Konstantinidis, C., 1987. A time simulation approach to the assessment of damage survivability of Ro/Ro cargo ships. Trans. Soc. Naval Arch. Mar. Eng. 95, 337–355.

van't Veer, R. and de Kat, O., 2000. Experimental and numerical investigation on progressive flooding in complex compartment geometries, In: Proceedings of the 7th International Conference on Stability of Ships and Ocean Vehicles, Launceston, Tasmania, Australia, 7–11 February 2000, pp. 305–321.

van't Veer, R., de Kat, O., and Cojeen, P., 2002. Large passenger ship safety: time to sink, In: Proceedings of the 6th International Ship Stability Workshop, New York, U.S.A, 13–16 October, 2002.

van't Veer, R., Peters, W., Rimpelä, A-L., and de Kat, J., 2004. Exploring the influence of different arrangements of semi-watertight spaces on survivability of a damaged large passenger ship, In: Proceedings of the 7th International Ship Stability Workshop, Shanghai, China, 1–3 November 2004.

Vassalos, D., Jasionowski, A., and Guerin, L., 2005. Passenger Ship safety – science paving the way, In: Proceedings of the 8th International Ship Stability Workshop, Istanbul, Turkey, 6-7 October 2005.

Woodburn, P., Gallagher, P., Letizia, L., 2002. Fundamentals of damage ship survivability. Trans. R. Inst. Naval Arch. 144, 143–163.